Title

Analyses of translation factors Dbp1 and Ded1 reveal the cellular response to heat stress to be separable from stress granule formation

Journal

Cell Reports, 43(12)

ISSN

2639-1856

Authors

Kuwayama, Naohiro

Powers, Emily Nicole

Siketanc, Matej

et al.

Publication Date

2024-12-01

DOI

10.1016/j.celrep.2024.115059

Peer reviewed

Published in final edited form as:

Cell Rep. 2024 December 24; 43(12): 115059. doi:10.1016/j.celrep.2024.115059.

Analyses of translation factors Dbp1 and Ded1 reveal the cellular response to heat stress to be separable from stress granule formation

Naohiro Kuwayama[1,6], **Emily Nicole Powers**[1,6], **Matej Siketanc**[3], **Camila Ines Sousa**[1], **Kendra Reynaud**[1], **Marko Jovanovic**[2], **Maria Hondele**[3], **Nicholas Thomas Ingolia**[1,4,5], **Gloria Ann Brar**[1,4,5,7,*]

[1]Department of Molecular and Cell Biology, University of California, Berkeley, Berkeley, CA 94720, USA

[2]Department of Biological Sciences, Columbia University, New York, NY 10027, USA

[3]Biozentrum, Center for Molecular Life Sciences, University of Basel, 4056 Basel, Switzerland

[4]California Institute for Quantitative Biosciences (QB3), University of California, Berkeley, Berkeley, CA 94720, USA

[5]Center for Computational Biology, University of California, Berkeley, Berkeley, CA 94720, USA

[6]These authors contributed equally

[7]Lead contact

SUMMARY

Ded1 and Dbp1 are paralogous conserved DEAD-box ATPases involved in translation initiation in yeast. In long-term starvation states, Dbp1 expression increases and Ded1 decreases, whereas in cycling mitotic cells, Dbp1 is absent. Inserting *DBP1* in place of *DED1* cannot replace Ded1 function in supporting mitotic translation, partly due to inefficient translation of the *DBP1* coding region. Global translation measurements, activity of mRNA-tethered proteins, and growth assays show that—even at matched protein levels—Ded1 is better than Dbp1 at activating translation, especially for mRNAs with structured 5′ leaders. Heat-stressed cells normally downregulate translation of structured housekeeping transcripts and halt growth, but neither occurs in Dbp1-expressing cells. This failure to halt growth in response to heat is not based on deficient stress granule formation or failure to reduce bulk translation. Rather, it depends on heat-triggered loss

*Correspondence: gabrar@berkeley.edu.

AUTHOR CONTRIBUTIONS

N.K. designed, executed, and analyzed experiments and edited the manuscript. E.N.P. designed, executed, and analyzed experiments and contributed to writing the manuscript. C.S., M.S., M.J., and M.H. designed, executed, and analyzed experiments and edited the manuscript. N.T.I. assisted in experimental design and manuscript editing. G.A.B. designed and analyzed experiments and wrote the manuscript.

DECLARATION OF INTERESTS

The authors declare no competing interests.

SUPPLEMENTAL INFORMATION

Supplemental information can be found online at https://doi.org/10.1016/j.celrep.2024.115059.

of Ded1 function mediated by an 11-amino-acid interval within its intrinsically disordered C terminus.

In brief

Kuwayama and Powers et al. reveal differences in function for two related RNA remodelers. Dbp1 is poor at stimulating translation, but, when expressed instead of Ded1, it prevents cells from halting growth upon heat stress. This depends on a short disordered Ded1 region but not stress granule formation or reduced translation.

Graphical Abstract

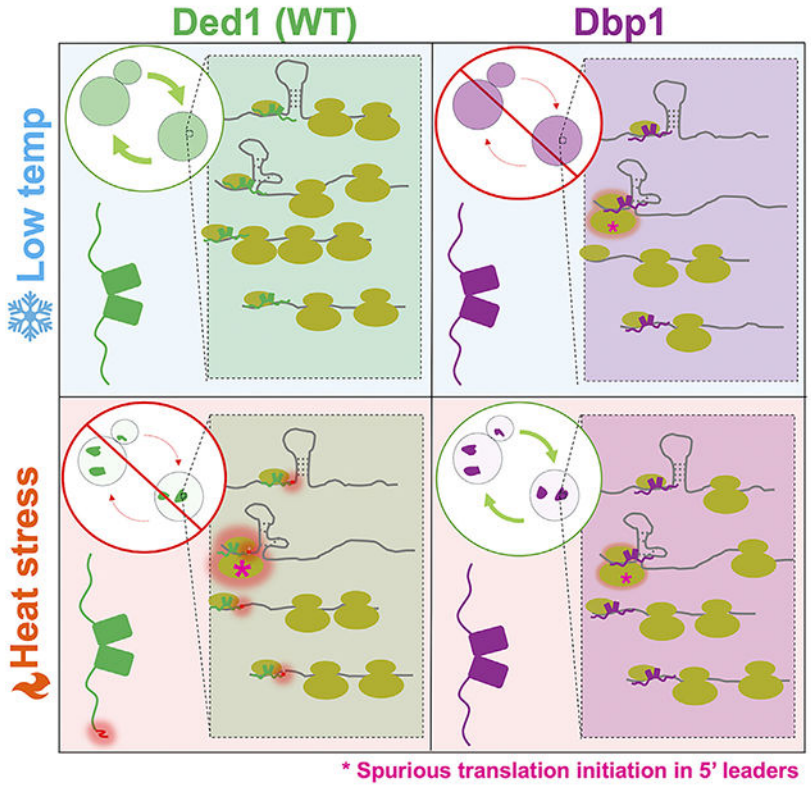

INTRODUCTION

DEAD-box ATPases, named for a motif involved in their catalytic activity, are a conserved and abundant class of proteins with critical roles in the regulation of RNA.[1–4] They function as helicases, or more accurately as non-processive remodelers of RNA secondary structure, which aids them in functions including mRNA decay, ribosome biogenesis, mRNA export, and translation initiation. Based on the current understanding of these proteins' molecular functions, we will not refer to them by the common phrase "DEAD-box helicase" but rather by "RNA remodeler" or "DEAD-box ATPase."

Translation initiation—the process by which start codons within mRNAs are chosen and decoded by the ribosome—requires two essential DEAD-box ATPases in yeast, Ded1 (DDX3 in mammals) and eIF4A[1,4,5] (Tif1/2 in yeast; DDX2A/B in mammals). This process is proposed to occur predominantly by the scanning mechanism, beginning with binding at an mRNA 5′ end by the 43S preinitiation complex (PIC)—including the 40S ribosomal subunit, initiator methioninyl tRNA, GTP, and initiation factors—directed by 5′ cap-bound eIF4G, eIF4E, and eIF4A (referred to together as eIF4F) to form the 48S PIC. 48S complexes scan the mRNA in a 5′ to 3′ direction, traversing the 5′ leader until a suitable start codon is found.[6] Ideal start codons are AUGs with optimal sequence context, but AUGs in poor context or non-AUGs are chosen in some instances.[6–9] Scanning may be enabled by eIF4A and Ded1, which help to resolve secondary structures that impede progress of the PIC.[10–15]

eIF4A appears to promote translation initiation on all mRNAs, whereas Ded1 has been shown to have particular importance for promoting initiation at start codons downstream of highly structured 5′ leaders,[13,14,16,17] a role shared by its human homolog DDX3.[18] Diminished function of Ded1 leads to lower translation levels and reduced growth rates.[13,19] Ded1 associates with PICs through its interactions with each of the components of eIF4F.[11,14,15,17,20,21] Cells deficient for Ded1 display spurious translation initiation at a subset of near-cognate codons within 5′ leaders and particularly at sites upstream of structured regions of mRNA.[10,22]

Paradoxically, Ded1 overexpression is associated with repression of translation and stress granule formation, which is also seen in specific conditions, including heat stress in the absence of its overexpression.[17,22–25] Ded1 is a core component of stress granules, and its role in this context has been linked to the conserved cellular outcome of reduced growth in response to stress, although how this happens is unclear. By one model, condensation of Ded1 into stress granules effectively reduces the pool of soluble Ded1 available to enable translation initiation. Another model posits that Ded1 pulls its mRNA targets into stress granules, thus repressing their translation. Data in support of the first model include the observation that cells deficient for Ded1 and cells exposed to heat shock (a condition that leads to stress granule formation) downregulate translation of a similar set of transcripts.[25,26] In support of the second model is the observation that structured Ded1-dependent mRNAs have been observed in Ded1 condensates.[25] In support of both models is the near-perfect correlation among four features of the cellular response to stress: (1) the presence of Ded1 in stress granules, (2) reduced bulk translation, (3) stress-induced shifts in what is translated, and (4) reduced cell growth.[25,27] At odds with both models are recent findings that stress granules may not repress translation.[28,29]

Dbp1 is a paralog of Ded1 with a core amino acid sequence that is 82.6% identical to Ded1 and more divergent N- and C-terminal sequences[30–32] (Figure 1A). Ded1's intrinsically disordered N and C termini contain its eIF4F-binding sites.[11,15,17,21,30,33] Whether equivalent sites exist within Dbp1 termini is not known. Dbp1 can support growth in cells lacking Ded1 when expressed at very high levels,[31,32,34] but it is unclear whether it has any unique functional characteristics.

Dbp1 is nonessential and very lowly expressed under standard laboratory growth conditions. *In vivo* analysis of Dbp1 function has been challenging due to a dearth of conditions in which it is known to be expressed and an unexpected side effect associated with its deletion via cassette-based genomic replacement. We recently showed that this genome-editing strategy, which was used to make all published yeast strains deleted for *DBP1*,[30,32,34–36] causes strong translational downregulation of *DBP1*'s neighboring open reading frame (ORF), encoding a mitochondrial ribosomal protein. This off-target effect results in downregulation of cytosolic translation and was responsible for all mutant phenotypes observed in otherwise wild-type (WT) cells deleted for *DBP1* via cassette replacement.[37] One condition in which Dbp1 is highly expressed is meiosis, a differentiation program that produces haploid gametes from diploid cells. Entry into meiosis is driven by the absence of fermentable carbon sources and low nitrogen in budding yeast. Timely induction of this differentiation program promotes cell survival, as the resultant spores are highly fortified and resistant to stressors (reviewed elsewhere[38–40]). If a growing yeast population depletes its available nutrients and continues to divide mitotically, cells will perish unless growth is halted or differentiation is stimulated.

The discovery that mutant phenotypes found in previous studies of *dbp1Δ* cells were likely to be complicated by off-target effects, together with strong upregulation of Dbp1 expression in specific conditions, including meiosis, motivated us to investigate its function. Our studies were designed to investigate Dbp1 and Ded1 roles *in vivo*, at endogenous and equivalent levels, given the known concentration dependence of Ded1's translation-activating and -repressing roles. We also avoided use of temperature-sensitive alleles to prevent confounding effects of temperature on translation and designed new tags to preserve protein function. We show that replacement of Ded1 with equivalent levels of Dbp1 in exponentially growing cells leads to enhanced translation in 5′ leaders, poorer translation of mRNAs with highly structured 5′ UTRs, less efficient translation-stimulating activity when tethered to a model transcript, and poorer ability to support cell growth at low temperatures (a condition in which mRNA structures would be expected to be stabilized). These findings all argue that Dbp1 is less effective at stimulating translation than Ded1, dependent on its intrinsically disordered termini.

Cells expressing Dbp1 in place of Ded1 are also unable to halt growth at high temperatures —a Ded1 role previously attributed to translation inhibition by stress granule formation —also dependent on the protein's intrinsically disordered terminal regions. We find that heat-stressed cells expressing Dbp1 in place of Ded1 are deficient at inhibiting translation of housekeeping genes with structured 5′ leaders but that this is not a result of deficiency in stress granule formation or reduction in bulk translation. Instead, heat-induced changes that are specific to Ded1preferentially impact translation of a small structured subset of mRNAs. The key role of Ded1 in the heat-stress response is, remarkably, conferred by an interval of only 11 amino acids at its C terminus. Based on these findings, we propose that a two-pronged response to heat stress occurs: Ded1 undergoes a heat-induced change in function that is responsible for reducing translation of structured housekeeping transcripts and dramatically reducing cell growth, but this effect is separable from stress-granule formation and a general decrease in total translation.

In conditions of rapid growth, Ded1 is expressed and Dbp1 is not, allowing cells to maximally activate translation and rapidly halt cell growth in response to changes in external conditions. Dbp1 expression is upregulated and Ded1 downregulated specifically in several conditions of long-term nutritional stress, suggesting that a “low-performance” DEAD-box RNA remodeler like Dbp1, which is more stress insensitive and less efficient at driving translation, is preferred under conditions in which rapid responses to changes in environment are not advantageous.

RESULTS

Dbp1 and Ded1 expression are inversely correlated

Ded1, but not Dbp1, is highly translated during mitotic exponential growth (Figure S1A). Dbp1 is translated at a level that is 69-fold higher in meiotic relative to mitotic cells, whereas most translation-associated DEAD-box ATPases, including Ded1, decrease in meiosis[10,41] (Figure S1A). Dbp1 and Ded1 protein abundances follow a similar trend to their translation, with Ded1 decreasing to roughly half its mitotic levels in midmeiosis[10] (Figures 1B and 1C). Dbp1 protein is typically undetectable in mitotic cells (Figure 1B). mRNA abundance is also very low, at ~2 reads per kilobase million (RPKM; Figure S1B;[41,42]) by mRNA sequencing (mRNA-seq), equivalent to *SPO11* and *DMC1*, two transcripts characterized as restricted from mitotic expression. *DBP1* translation and protein increase in meiosis to levels comparable to Ded1[41,42] (Figures S1A, 1B, and 1C). This regulation occurs through increased mRNA abundance via transcriptional induction, rather than reduced mRNA degradation, as *DBP1* mRNA is not transcribed in mitotic cells.[43]

DBP1 mRNA is expressed in several non-meiotic conditions, including “post-diauxic” growth following exhaustion of a fermentable carbon source, stationary phase (driven by nutrient exhaustion), and long-term nitrogen deprivation[44] (Figures 1D and S1B). Notably, in all cases in which Dbp1 expression is induced, Ded1 expression decreases. Dbp1 expression is not induced in response to the majority of characterized cellular stresses, including long-term temperature shifts, or acute stressors.[44] Increased Dbp1 expression and reduced Ded1 expression thus appear to be associated with long-term states of cellular maintenance in limiting nutrient conditions.

An increase in translation within 5′ leaders, particularly at non-AUG codons, occurs when Ded1 function is compromised, attributed to inefficient disruption of 5′ mRNA structures during PIC scanning.[10,45,46] Meiotic cells also display increased 5′ leader translation and non-AUG initiation[10,41,47] (Figure S1C). This led us to hypothesize that Dbp1 might exhibit poorer ability to support translation initiation than Ded1, potentially contributing to the enhanced translation within 5′ leaders in meiotic cells (Figure S1C).

Genomic replacement of *DED1* with *DBP1* reveals their ORF-dependent differential translation

We asked whether physiological levels of Dbp1 could support mitotic exponential growth, a condition in which Ded1 has defined functions. We create an unmarked deletion of *DED1* (*ded1Δ*) and genomically integrated a construct homozygously in diploid cells that contained

either the *DED1* or *DBP1* ORF under control of the *DED1* promoter, 5′ leader, 3′ UTRs, and terminator (Figure 1E). Untagged Ded1 produced by this strategy supported normal mitotic growth (Figures 1F and S1D). Untagged Dbp1 did not, causing cell doubling time to be increased by roughly 20% (Figures 1F and S1D). This reduced growth rate was associated with decreased bulk translation, as assessed by ^{35}S amino acid incorporation and polysome gradient analysis (Figures 1G and 1H). This suggested that Dbp1 was less effective at supporting translation than Ded1 in mitotic cells.

The bulk translation defect seen when Ded1 is replaced by Dbp1 could be because Ded1 is required to promote translation of specific transcripts that support rapid growth and ultimately high translation. Reduced translation would thus be an indirect result. Alternatively, Dbp1 could have a lower capacity than Ded1 to stimulate translation initiation on all transcripts, thus supporting lower bulk translation and slower growth than mitotic cells expressing Ded1. To investigate these possibilities, we performed ribosome profiling and mRNA-seq in triplicate on Ded1- versus Dbp1-expressing cells (Files S1 and S2A). Increased ribosome density in the region 100 nucleotides (nt) upstream of annotated ORF start codons was observed in cells expressing Dbp1 compared to Ded1 (Figure 1I), suggesting that Dbp1 could not disrupt the 5′ leader structures that impede scanning and robust initiation to the degree that Ded1 does. Additionally, many genes displayed differences in mRNA levels, translation rates, and translation efficiencies (TEs; TE = ribosome footprint RPKM values/mRNA RPKM) in Dbp1- and Ded1-expressing cells (Figures S2B–S2G).

The major surprise from this dataset, however, was that, despite matched regulatory regions driving Dbp1 and Ded1 expression, translation of *DBP1* was lower than translation of *DED1* (Figures 2A and S2H). *DBP1* mRNA levels were 2.4-fold higher than that of *DED1* (Figure 2A), resulting in a TE for *DBP1* that was less than half of that observed for *DED1* (Figure 2B). As expected based on translation rates (Figure 2A), Dbp1 protein was present at a lower abundance than Ded1, as assessed by western blotting (Figure 2C). To increase Dbp1 levels, we inserted either one or two extra copies of the *DBP1* ORF flanked by *DED1* regulatory elements at the *TRP1* locus (1.5× Dbp1 and 2× DBP1; Figures 2D and S3A). When twice as many copies of *DBP1* ORF were supplied as *DED1* ORF—flanked by *DED1* regulatory regions in both cases—protein levels between the two internally tagged proteins were indistinguishable by western blotting (Figure 2E). Higher Dbp1 protein levels also rescued mitotic growth to match growth of Ded1-expressing cells (Figures S3B and S3C).

Loss of Dbp1 expression in meiosis leads to upregulation of Ded1 expression

Given the enhanced expression of Dbp1 in meiosis (Figures 1B–1D), we examined the effects of Dbp1 loss in this context. A markerless *dbp1Δ* cell line does not appear to exhibit off-target effects[37] and displays no mitotic growth or translation defect, consistent with the lack of Dbp1 expression under these conditions. Surprisingly, we also observed little defect in meiotic progression (Figure S4A) or meiotic translation (Figures S4B and S4C) in cells lacking Dbp1. Consistently, mRNA-seq and ribosome profiling of WT and *dbp1Δ* cells at early (3 h) and mid-meiotic (6 h) time points revealed few differences genomewide (Figures S4D–S4F; File S3). These results were unexpected, given the apparent sensitivity of mitotic

growth to DEAD-box ATPase level (Figures 1F–1H, 2C, 2E, S3B, and S3C) and the large contribution of Dbp1 to the Ded1/Dbp1 pool in meiosis (Figures 1B and 1C). Examination of *DED1* expression provided an explanation: *dbp1Δ* cells showed a significant increase in translation of *DED1* (Figures S4G and S4H), suggesting that meiotic cells compensate for low Dbp1 levels by upregulating production of Ded1.

Dbp1 cannot support robust cell growth at cold temperatures

Mitotic cells expressing an equivalent amount of Dbp1 instead of Ded1 display no measurable growth defect at standard laboratory growth temperatures (30°C; Figure S3C) and meiotic cells expressing a small amount of Ded1 instead of Dbp1 (Figure S4G) displayed no measurable defect completing meiosis (Figure S4A), suggesting that the functions of the two proteins are largely overlapping. We hypothesized, however, that differences in their functions may be unmasked by growing cells expressing either Dbp1 or Ded1 at low or high temperatures. At low temperatures, mRNA structures should be stabilized, demanding particularly high RNA remodeling activity. We observed that, although cells carrying four copies of *DBP1* (2×; Figure 2D) driven by *DED1* regulatory regions grew as well as those expressing Ded1 at 30°C, Dbp1 expression conferred a strong growth defect at 18°C (Figure 3A). This defect suggested poorer performance of Dbp1, relative to Ded1, in activating translation at cold temperatures. Consistently, this effect was more severe in diploid cells housing only two copies of *DBP1* (1×; Figure 3A) and this was not merely a result of slower growth, as cells lacking *RPL26B* displayed a similar mitotic growth defect to *1X DBP1* cells at 30°C, but a much less severe growth defect at 18°C (Figure 3B).

Epitope tags at Ded1's N and C termini can impact its function

The relative growth defect at 18°C caused by Dbp1 expression during mitotic growth, compared to Ded1, was seen whether these proteins were internally 3V5-tagged or untagged (Figures 3A and 3C). N- or C-terminal 3V5 tags on Ded1, however, resulted in reduced growth of cells compared to untagged controls at 18°C (Figures 3C and S1E). This is important, given that most studies examining Ded1 function have relied on terminally tagged versions of this protein. Ded1's eIF4F-binding sites are at its termini, which could be partly occluded by use of N- and C-terminal tags. We used internally tagged proteins for most subsequent experiments, based on comparison of growth of cells carrying tagged Ded1 and Dbp1 (Figures S1E and S1F).

Ded1 is more efficient at associating with ribosomes than Dbp1

Why is Dbp1 poor at supporting cold-temperature growth? This could be based on worse association of Dbp1 with scanning ribosome subunits or poorer activity in stimulating translation initiation. To test the first possibility, we performed mass spectrometry of ribosomes isolated from mitotic and meiotic cells (Figure 4A; time points in Figure S1A). We analyzed the translating ribosome fractions, rather than 40S species, because most translation initiation occurs on mRNAs that are already being translated and thus translating fractions should contain more PICs than sub-80S fractions (Figure 4A top cartoon). We compared tandem mass tag (TMT)10 mass spectrometry values for ribosome-associated fractions to those for matched total extract (Figure 4A; File S4). For general translation

factors (such as eIF4A), the greater total protein in mitotic cells corresponded generally with greater protein associated with mitotic ribosomes. This was also true for Ded1 (Figure 4A). In the case of Dbp1, much higher total protein and translation-associated protein was seen, as expected, in meiotic cells than mitotic cells. However, even at time points for which Ded1 and Dbp1 protein levels were equivalent in total extract, Dbp1 was found in fractions associated with translation at substantially lower levels than Ded1 (Figure 4A).

Tethering experiments reveal reduced translation activation capacity for Dbp1

We next examined the ability of Dbp1 to enhance translation, using an mRNA tethering assay.[48,49] We fused either Dbp1, Ded1, or a control Halo-tag to the λN coat protein in cells expressing a YFP reporter mRNA containing five boxB hairpins in its 3′ UTR (Figure 4B). An RFP reporter housing five PP7 hairpins in its 3′ UTR was also expressed in cells as a control, and YFP to RFP ratio was assessed by flow cytometry. Tethering of Ded1 to the reporter mRNA increased the YFP/RFP ratio in mitotic cells, indicating that it behaves like a translational activator (Figures 4B and 4C). This is consistent with published data, which found an N-terminal fragment of Ded1 to be among the most translationally activating protein regions.[49] Dbp1 stimulated expression of the YFP reporter, but the magnitude of activation was lower than with Ded1 (Figure 4C). This effect was translational, as no difference in mRNA levels between the two constructs was observed (Figure S5A). Chimeric DEAD-box ATPases were also analyzed, by swapping the N-terminal, core, and C-terminal regions of Ded1 and Dbp1.[30] The Nterminus of Ded1, containing its eIF4E- and eIF4A-binding sites, was key to maximum translational activation by this assay (Figures 4B and 4C).

The in-cell tethering approach allows assessment of translational regulation under different *in vivo* conditions. Because Dbp1 is upregulated and Ded1 is downregulated during meiosis, we wondered whether Dbp1 may be more effective at activating translation in this cellular context. This was not the case. Meiotic cells displayed highly similar translational activation profiles to mitotic cells, with Ded1 leading to enhanced translation activation compared to Dbp1, and Ded1's N terminus playing a particularly important role (Figures 4B and 4D). In meiotic cells, as opposed to mitotic, Ded1's N terminus alone could not fully support translational activation to the level seen with full-length Ded1, and a contribution of Ded1's C terminus alone was also seen (Figures 4B and 4D). No relationship was observed between protein level and degree of translational activation, suggesting that the DEAD-box ATPases were in excess of reporter mRNA (Figures S5B and S5C). These experiments revealed that Dbp1 is inherently less effective at stimulating translation than Ded1, even when artificially recruited to its mRNA target, and that this difference is driven by its N and C termini.

Ded1 replacement with Dbp1 drives increased 5′ leader translation in mitosis

We performed ribosome profiling of diploid cell lines expressing Ded1, 1× Dbp1, or 2× Dbp1 (Figures 2D and S3A; File S2). Cells lacking Ded1 (*ded1-ts*) accumulate ribosome footprints in 5′ leaders, reflecting spurious translation initiation as a result of PICs stalling at structured 5′ regions during the scanning process.[10] Similar accumulation of 5′ leader ribosome footprints was seen when low (1×) or Ded1-matched (2×) levels of Dbp1 were expressed, compared to cells expressing Ded1 (Figures 1I, 4E, and 4F). This further supports

the model that Dbp1 is less effective at stimulating proper translation initiation than Ded1, and this was apparent for both a subset of highly expressed transcripts (e.g., *DHH1* in Figure 4E) and when data for annotated ORFs were analyzed in aggregate by metagene analysis (Figures 1I and 4F). The effect could not be explained by an indirect effect of decreased bulk translation, as increased ribosome occupancy in 5′ leaders was not seen in cells lacking *RPL26B*, a condition that results in low bulk translation, equivalent to the 13 Dbp1 cell line[50] (Figure 4F).

mRNAs with structured 5′ leaders are more efficiently translated by Ded1 than Dbp1

Ded1 function is important for stimulating translation generally, but its loss impacts transcripts most that are structured and contain long 5′ leader regions.[10,12,13,25,26,32] Our data that Dbp1 shows poorer association with ribosomes than Ded1 (Figure 4A), is less effective at stimulating translation (Figures 4B–4D), and that its expression in mitotic cells leads to enhanced translation within 5′ leaders (Figure 4F) all suggest that cells with mitotic replacement of Ded1 with Dbp1 behave as though they express a partial loss-of-function allele of *DED1*. If true, we would expect mitotic cells expressing a Ded1-matched level of Dbp1 to show reduced translation of mRNAs with structured 5′ leaders, compared to Ded1-expressing cells. To assess this, we examined the mRNA-seq and ribosome profiling datasets, comparing cells expressing either Ded1, low levels of Dbp1, or levels of Dbp1 that were matched to Ded1 (Figures 2D and S5D; File S2). Few differences in mRNA or translation levels were observed when comparing Dbp1- to Ded1-expressing cells (Figures S5E–S5G), and the changes that were seen did not correspond to those that are indicative of low overall translation levels[50] (Figure S5H), supporting the model that they were instead a result of differences in specificity of Ded1 versus Dbp1 in promoting translation initiation.

Using hierarchical clustering of all data, we identified three clusters of interest. Two (1 and 2, Figure 5A) contained mRNAs that were translated at a higher level when Dbp1 was expressed in place of Ded1. One (3, Figure 5A) contained mRNAs that were translated at a higher level when Ded1 was expressed rather than Dbp1. The degree of difference in translation profiles between cells expressing the two RNA remodelers in all three clusters was mild, with the 249 mRNAs in the two Dbp1-enhanced clusters showing only a 34% increase on average of ribosome footprints in 2× Dbp1 cells relative to those expressing Ded1 (excluding *DBP1* itself). Similarly, the 158 mRNAs in the Ded1-enhanced cluster showed only a 20% average increase in translation in cells expressing Ded1 compared to 2× Dbp1-expressing cells (excluding *DED1* itself). The mRNAs that showed enhanced translation when Ded1 was expressed, relative to Dbp1, were highly enriched for structured 5′ leaders, as assessed by *in vivo* mRNA structure determination by DMS-MaP-seq[51] (Figure 5B). This is consistent with reports that Ded1 is important for translation of 5′ leaders with predicted structure, based on minimum-free-energy analyses[10,12,25,32] (Figure 5C) and our data that Dbp1 is less effective at driving translation initiation than Ded1 (Figure 4).

Dbp1 cannot suppress cell growth at high temperatures

The halting of cell growth in response to high temperature is a widespread normal feature of eukaryotic cells. Surprisingly, in contrast to the WT situation in Ded1-expressing cells,

cells expressing Dbp1 were unable to halt growth at 37°C, whether Dbp1 was untagged, N- or C-terminally tagged, or internally tagged (Figures 3A–3C and S1E). Stress conditions leading to halting of cell growth also lead to Ded1 localization in stress granules, bulk reduction in translation, preferential repression of translation of "housekeeping" mRNAs, and reduced cell growth,[17,25,27] but the relationships between these features has been difficult to disentangle. We reasoned that comparing them in Dbp1- and Ded1-expressing cells might be informative in explaining how cells modulate translation to halt growth under stressful conditions.

Dbp1-expressing cells are deficient at heat-induced suppression of housekeeping gene translation

The condensation of Ded1 into stress granules in response to heat stress is proposed to lead to poor cell growth under such conditions.[25] It has also been proposed that other translation initiation factors, including eIF4A, dissociate from mRNAs in response to stress, and this can compound the effects of Ded1 loss of function caused, at least in part, by its condensation into stress granules.[26] Our observation that Dbp1-expressing cells grow well at 37°C, whereas Ded1-expressing cells do not (Figure 3A), suggested that Dbp1 may not be able to function in the proposed stress-granule-mediated translational repression that is thought to reduce cell growth at high temperatures.

We performed ribosome profiling of mitotic cells grown at 30°C and 37°C, and expressing either Ded1 or Dbp1 driven by *DED1* regulatory regions (File S5). Hierarchical clustering of Ded1-expressing cells (effectively WT cells) revealed a large cluster of 1,757 transcripts displaying increased translation at 37°C, compared to 30°C, as well as a cluster of 618 transcripts displaying reduced translation (Figure S6A). Consistent with analyses using predictions of mRNA structure,[25] the 5′ leaders for transcripts whose translation was downregulated with heat were more structured *in vivo* than average, whereas those that were upregulated with heat were less structured *in vivo* than average (Figure 5D). Also consistent with previous findings, downregulated transcripts included housekeeping genes (Table S1).

We next compared ribosome profiling data from Ded1- vs. Dbp1-expressing cells at 37°C (File S5). Hierarchical clustering revealed two clusters of transcripts (1 and 2, Figure 5E) whose translation was higher in Ded1-expressing cells and one cluster (3, Figure 5E) whose translation was higher in Dbp1-expressing cells. The latter group was highly enriched for the group of primarily housekeeping genes that were normally downregulated at 37°C (Figure S6A, lower cluster; Fisher exact test $p < 0.000001$; Tables S1 and S2). The genes with higher translation in Dbp1-expressing cells relative to Ded1-expressing cells at high temperature also had highly structured 5′ leaders (Figure 5F). Together with the observation that the transcripts that are most downregulated in cells lacking Ded1 function are highly structured[25,32] (Figure 5C) and that Dbp1-expressing cells are unable to slow growth at high temperature (Figure 3A), these data support the model that high temperature selectively reduces Ded1 function (compared to Dbp1) in promoting translation of a relatively small number of transcripts with structured 5′ leaders and that this leads to poor cell growth (Figure 5G).

Dbp1 and Ded1 both form heat-induced stress granules and reduce bulk translation

We hypothesized that the inability of Dbp1-expressing cells to quell growth at high temperature resulted from their inability to form stress granules under these conditions. We constructed cell lines expressing matched levels of Ded1 and Dbp1 with internal GFP tags (Figures S6B and S6C), which recapitulated the high temperature sensitivity of Ded1-expressing cells but not Dbp1-expressing cells (Figures 3A, 3C, S6D, and S1E), and examined the subcellular distribution of both Ded1 and Dbp1. As expected, both Dbp1 and Ded1 were homogeneously cytosolic at 30°C (Figure 6A) and exposure of cells to high temperatures led to formation of puncta representative of stress granules in cells expressing Ded1 (Figures 6B and S6E). However, we observed comparable puncta in cells expressing Dbp1 at 37°C and higher temperatures (Figures 6E and S6E). In cells expressing both internally GFP-tagged Dbp1 and internally mScarlet-tagged Ded1, these puncta co-localized, indicating that the Dbp1 puncta were indeed stress granules (Figures 6C and S6F). Fluorescence recovery after photo bleaching (FRAP) analysis revealed similarly poor recovery in the case of both Dbp1 and Ded1 (Figures 6D and 6E), indicating that there is low mobility of both proteins within stress granules. Together, *in vivo* analyses suggest that, upon heat stress, both Dbp1 and Ded1 form stress granules that are comparable in their properties, but Ded1-expressing cells stop growing and display poor translation of structured housekeeping transcripts, whereas Dbp1 cells do not.

Polysome analyses of Dbp1- and Ded1-expressing cells revealed a profound decrease in bulk translation with heat stress in both cases, under conditions in which we observed stress-granule formation (Figures 6F and 6G). Together, our data separate four previously identified key features of the cellular response to heat stress—preferentially decreased translation of housekeeping transcripts, decreased cellular growth, decreased bulk translation, and stress-granule formation—into two groups. The former two are dependent on Ded1, whereas the latter two are not. This fortuitous observation also allows us to, in part, disentangle relationships of causality among these four features. For example, stress-granule formation or decreased bulk translation cannot underlie stress-induced quelling of growth because Dbp1-expressing cells display the first two but not the last.

Ded1 selectively exhibits a heat-stress-induced change in function

Stress-induced halting of growth is inherent to Ded1 function (Figure 3A). Given the proficiency of Dbp1-expressing cells to both grow during heat stress and their failure to repress structured housekeeping transcripts (Figures 5E and 5F), the very same class of transcripts that Ded1 preferentially promotes translation for under non-stress conditions (Figures 5A–5C), we considered the possibility that these changes resulted from heat-induced loss of Ded1 function. Metagene analysis of translation in Dbp1- and Ded1-expressing cells grown at 37°C indeed supported preferentially reduced Ded1 function with heat stress, revealing enhanced translation within 5′ leaders in Ded1-expressing cells (Figure 6H), reversing the pattern seen at 30°C (Figures 1I and 4F) and mimicking the effect seen with Ded1 loss of function.[10] This result indicates that, at high temperature, Ded1 is no longer superior to Dbp1 at stimulating translation.

To further probe the properties of Dbp1 compared to Ded1, we purified untagged proteins with chemical labeling of 1% of the protein for visualization. As previously reported for C-terminally tagged protein,[25,52] untagged Ded1 formed spherical condensates at 25°C that were dependent on RNA, but not on ATP (Figures 7A and S7G, right panels for 200 mM NaCl). Dbp1 formed *in vitro* condensates that resembled those formed by Ded1, except at low salt, where Dbp1 condensate formation was enhanced by RNA, whereas Ded1 condensate formation was reduced by RNA (Figures 7A and S6G, left panels). We next examined condensates for both Dbp1 and Ded1 at 37°C. It was previously observed that *in vitro* Ded1 condensates no longer resemble spherical liquid-like drops at high temperature.[25] We also observe a shift to irregularly shaped condensates for Ded1 at 37°C (Figures 7B, asterisks, and S6H). Dbp1 condensates, however, remained as smooth and spherical at 37°C as they were at 25°C, which was particularly clear in the presence of RNA (boxed panels in Figures 7B and S6H).

An 11-amino-acid C-terminal interval of Ded1 mediates its role in heat stress

Ded1 has been shown to undergo a tertiary structural change at high temperature that was proposed to underlie its condensation.[25] We purified untagged Ded1 and Dbp1 and analyzed them using nano-differential scanning fluorimetry (nanoDSF). These analyses indicated a similar thermal stability for Ded1 and Dbp1 (Figures S6I and S6J), indicating that the selective loss of Ded1 function at 37°C is unlikely to reflect gross structural changes, relative to Dbp1.

The high degree of growth seen in Dbp1-expressing cells at 37°C (Figures 3A and 3C) and the divergence of Dbp1 and Ded1's N- and C-terminal sequences (Figure 1A) led us to wonder whether Ded1's superior ability to activate translation relative to Dbp1 is based on its eIF4F-interacting intervals. If so, supplying Dbp1 with the six peptide segments shown to be important for Ded1 binding to eIF4A, eIF4E, and eIF4G should reduce Dbp1's ability to support robust growth at 37°C.[11,17] Indeed, cells expressing this Dbp1-eIF mutant displayed markedly reduced growth at 37°C compared to those expressing WT Dbp1 (Figures 7C and S6L). The C terminus of Ded1 is required for its robust interaction with eIF4G[17,20] and cells expressing C-terminally tagged Ded1 grow as well as those expressing Dbp1 at 37°C (Figures 3C and S1E). This led us to hypothesize that this region may alone confer the shift in Ded1 activity seen with heat stress. Indeed, growth and microscopy analyses confirmed that cells expressing C-terminally GFP- or mCherry-tagged Ded1 exhibited robust growth at 37°C, despite forming stress granules under these conditions (Figures 7D, 7E, and S6K). Cells expressing a version of Ded1 lacking only 14 amino acids from its C terminus, which removed most of the known eIF4G-interaction region,[17,20] displayed a growth defect relative to full-length protein when cells were grown at 18°C, suggesting reduced basal function (Figures 7C and S6L). Remarkably, these cells displayed robust growth at 37°C, with loss of only Ded1's 14 terminal amino acids phenocopying replacement of the entire protein with Dbp1 (Figures 7C and S6L). The three extreme C-terminal amino acids are identical in Dbp1 and Ded1 (Figures 7C), suggesting that the prior 11 amino acids of Ded1, within its intrinsically disordered eIF4G-binding region, are solely responsible for its normal heat-based shift in function.

How does the shift in Ded1's function repress translation of structured housekeeping transcripts in response to heat stress? One possibility is that Ded1 remains bound to its targets, which preferentially includes structured housekeeping transcripts, but is unable to support their efficient translation. In the absence of Ded1, Dbp1 would translate these mRNAs sufficiently well to support robust cell growth but the presence of Ded1 might sequester such mRNAs, or other initiation factors, from Dbp1. This model is consistent with data showing that structured housekeeping transcripts localize with Ded1 to stress granules in response to stress.[25] An alternative model is that the heat-induced shift in Ded1 function leads to its poor association with target transcripts. In this case, one would expect that cells expressing both Dbp1 and Ded1 would grow robustly at 37°C, similarly to those expressing only Dbp1. To distinguish between these models, we assayed growth of cells expressing Dbp1, Ded1, or both. We found that, as expected, the presence of Ded1 fully rescued the poor growth of Dbp1-expressing cells at 18°C (Figure 7F). However, the presence of Ded1 profoundly repressed growth of Dbp1-expressing cells at 37°C (Figures 7F and S6L). This result supports the model that the shift in Ded1's properties in response to heat stress does not affect its ability to interact with mRNAs or other translation factors, but renders it ineffective at promoting translation.

DISCUSSION

DEAD-box ATPases are abundant and common in eukaryotes, and they share many properties, including roles in regulating RNA and formation of *in vivo* condensates.[1] Our study, which used single-copy genomic replacement of *DBP1* and *DED1*, was the first to control for the levels of these RNA remodelers (commonly refered to as DEAD-box helicases) in assessing their function. We found that expression levels matter greatly and that, although Dbp1 can largely perform similar functions in translation initiation as Ded1,[31,32,34] it is less effective *in vivo* at activating translation and in halting translation of structured mRNAs in response to an external stressor. Both differences in Ded1 and Dbp1 activity can lead to dramatic effects on cell growth in non-standard laboratory conditions, such as at high and low temperatures (Figure 3).

Dbp1 is inherently less efficient at associating with ribosomes (Figure 4A), stimulating translation even when tethered to a transcript (Figures 4B and 4C), activating translation of highly structured 5′ leaders (Figures 5A and 5B), and bypassing suboptimal translation initiation codons within 5′ leaders[10] (Figure 4F). All of these results indicate that, even when comparing matched protein levels, Dbp1 is less effective at supporting translation than Ded1, dependent on the divergent N and C termini of the two proteins. Most of the defects seen in mitotic cells expressing an equivalent level of Dbp1 in place of Ded1 are modest, suggesting that, at least in exponential-phase mitotic growth, the two RNA remodelers are largely comparable in their translation-stimulating function. However, these functional differences may be of greater importance in suboptimal growth conditions. As one example, cells expressing *DBP1* in place of *DED1* at 18°C display a profound growth defect, potentially resulting from the more stable RNA secondary structures at low temperatures (Figure 3). A study of purified Dbp1 and Ded1 reported that Dbp1 displayed higher activity than Ded1 in promoting 40S binding and scanning.[32] There are many factors that differ between those experiments and ours, including the possibility of *in vivo* factors

that modulate DEAD-box protein activity and/or folding. However, it is worth noting that this study reports using N-terminal tags for purification. Given our finding that N-terminal tagging of endogenous Ded1 reduces its function (Figure S1E), it is possible that the tags that enabled this study also impacted its results.

Cells in diverse organisms, including yeast and human, display markedly reduced growth at high temperature, a response that is thought to support survival. Remarkably, yeast cells expressing Dbp1 in place of Ded1 no longer display this conserved response. The cessation of mitotic cell growth at high temperatures has been proposed to result from Ded1-driven formation of stress granules that result in poor translation of housekeeping mRNAs and enhanced translation of transcripts that encode stress-response factors.[17,25,27] Cells expressing Dbp1 fail to efficiently downregulate a set of mRNAs with highly structured leaders that are downregulated in heat-stressed cells expressing Ded1. However, Dbp1 forms stress granules under these conditions, representing the first case—to our knowledge—in which the growth effects of stress are unlinked from stress-granule formation.

Leveraging the similarity between Dbp1 and Ded1 allowed us to shed light on core aspects of Ded1 function that have been difficult to disentangle. Our data support the model that Ded1 function is central in the cellular response to heat stress.[25] They do not, however, support the model that slowed growth in response to stress results from lower levels of soluble DEAD-box ATPase available for promoting translation in cells with stress granules. Replacing Ded1 with Dbp1 does not block the ability of cells to form stress granules or to globally reduce translation but does prevent efficient repression of structured housekeeping transcripts and the halting of cell growth. Thus, stress-granule formation, per se, is not required for these latter two features of the heat-stress response (Figures 7G and 7H).

What is the nature of the shift in Ded1 function that occurs at high temperature? Although a dramatic change in Ded1 tertiary structure has been reported at high temperature,[25] we do not believe such a wholesale structural change in Ded1 is the likely driver of its loss of function in response to heat stress for several reasons. First, these gross Ded1 structural changes are only seen to begin above 40°C,[25] whereas its shift in function and *in vitro* condensate appearance can be seen at 37°C (Figures 3A, 3C, 5D–5F, 6H, 7A–7F, and S6H). Second, a short (11-amino-acid) interval of Ded1 is necessary and sufficient for heat-induced halting of cell growth (Figures 7C and 7G) and is situated in Ded1's intrinsically disordered C terminus (Figure 1A), which would not be expected to affect its tertiary structure. Third, the shift in Ded1 function can be mimicked by adding GFP or 3V5 to its C terminus, neither of which is predicted to affect its core structure (Figures 3C, 7D, and 7E). Finally, our comparison of Dbp1 and Ded1 structure at high temperature does not indicate major differences in thermal stability (Figures S6I and S6J), despite dramatic functional differences. The 11-amino-acid region of Ded1 that determines its heat-sensitive shift in function is within its eIF4G-binding region.[17,20] One possibility is that these 11 amino acids undergo a heat-induced change that affects Ded1's interaction with eIF4G. This could be akin to the change in eIF4G's eIF4A-interacting domain that occurs at high temperature.[53] It is interesting that the shift in Ded1 function at high temperature is dominant (Figure 7F), suggesting that the presence of Ded1 restricts Dbp1 from accessing Ded1's preferred transcripts. This may be through persistent direct binding between Ded1 and targets at high

temperature. Alternatively, it could be indirect, through sequestration or inactivation of a factor (such as eIF4G) that is important for translation of these targets.

Together, our data and recent data from others allow a coherent model for the cellular response to heat stress. We argue that this response is two-pronged: (1) changes in eIF4G-4A interactions may lead to reduced bulk translation[53]; (2) a short C-terminal peptide in Ded1 causes its reduced function at high temperature and restricts translation of structured housekeeping transcripts (Figures 7G and 7H). This subtle shift in translation of a subset of mRNAs seems to be responsible for the quelling of cell growth seen with heat stress. Stress granules do not seem to drive the second, Ded1-dependent pathway; whether they result from or contribute to the first pathway remains unclear.

Our results comparing the functions of the two DEAD-box RNA remodelers provide key insight into their relative functions, supporting the model that Ded1 is a “high-performance” initiation factor, perhaps akin to an F1 vehicle. It can support maximal translation and cell growth, and is highly stress responsive, allowing cells to quickly shift what they translate and halt growth. Dbp1 is less powerful at both activating and braking functions, more like a family sedan. So what is Dbp1’s purpose in cells? The conditions in which it is expressed may provide insight (Figures 1D and S1B). All reflect chronic stress conditions, in which cellular resources are limiting for timespans that exceed typical mitotic doubling times.[44] In the case of meiosis, bulk translation levels are lower than during mitotic exponential growth[41], and thus an RNA remodeler that is only moderately efficient at stimulating translation may be tolerated, perhaps even preferable. It may also not be advantageous for cells to stop meiotic progression in response to an acute external stressor, as they cannot return to mitotic growth after a restriction point relatively early in the meiotic program. Halting translation would simply delay gamete formation without hope of improved conditions.

The increase in 5′ leader translation seen in mitotic cells expressing Dbp1 in place of Ded1 phenocopies the increase in translation initiation at near-cognate codons in 5′ leaders seen in cells deficient for Ded1 function. Spurious translation initiation would be expected to generally decrease the overall efficiency of synthesis of proteins encoded downstream of these sites but it could also offer an advantage under certain circumstances. We recently showed that translation initiation within 5′ leaders is common in meiosis and can result in production of alternative N-terminally extended protein isoforms.[41,47,54] Such alternative isoforms are known to be important in some cases, and can function in dually targeting a protein product to an additional subcellular location (akin to[55]). The enhanced near-cognate initiation seen in meiosis is in part dependent on low eIF5A expression,[47] but the low Ded1 and high Dbp1 expression under these conditions may also contribute. The set of factors that drive this increase in production of noncanonical protein isoforms diversifies the proteome in meiosis and may support cellular functions that are important in this cellular context.

Limitations of the study

Detection of Dbp1 and Ded1 relied on tagging and, although we tested tagged strains for growth functions, any epitope tags may interfere with normal cellular roles in ways that are difficult to predict. In the case of the tethering experiments (Figures 4B–4D), C-terminal

tags were used, which reduce Ded1 function (Figure S1E) under these conditions and may underestimate the difference between Dbp1 and Ded1 function in this assay.

RESOURCE AVAILABILITY

Lead contact

Requests for further information and resources should be directed to and will be fulfilled by the lead contact, G. Brar (gabrar@berkeley.edu).

Materials availability

All unique reagents generated in this study will be made available on request, but we may require a payment and/or a completed materials transfer agreement if there is potential for commercial application.

Data and code availability

- Processed global data are provided in Files S1–S5. Raw mRNA-seq and ribosome profiling data are deposited at NCBI GEO with accession numbers GSE262933, GSE262934, and GSE262935.
- This paper does not report original code.
- Any additional information required to reanalyze the data reported in this paper is available from the lead contact upon request.

STAR★METHODS

EXPERIMENTAL MODEL AND STUDY PARTICIPANT DETAILS

Yeast strains are *Saccharomyces cerevisae* in the SK1 background.

METHOD DETAILS

Strain construction—All strains used in this study were of derivatives of Saccharomyces cerevisiae of strain background SK1, outside of those used for tethering experiments which were of BY or hybrid SK1 and BY background. Strain genotypes can be found in File S6. All genome edited transformants were backcrossed at least once prior to use. To construct the unmarked *ded1Δ* allele, we first cloned a single copy of the *DED1* ORF C terminally tagged with 3v5 and ~1kb of upstream and downstream regulatory sequence into a single integration vector and inserted it into the *LEU2* locus. This strain was then transformed with a plasmid encoding Cas9 and a sgRNA targeting the C terminus of *DED1* that is unable to target the C terminally tagged Ded1 allele inserted at the *LEU2* locus. The Cas9 editing plasmid was transformed alongside a linear repair template that deletes the *DED1* ORF. The *ded1Δ* was backcrossed and all subsequent rescue strains were created by transforming a wild-type strain with the *LEU2* integrated helicase, backcrossing, then crossing the rescue allele to the ded1Δ. Internal helicase tags were designed by finding sites that tolerated insertions within the Ded1 helicase by looking at sequence alignments to homologs from other species. Possible insertion sites were confirmed to be un-structured and surface exposed by examining their location on a published Ded1 structure. Tag functionality was

determined by comparing the growth of tagged and untagged helicases under all growth conditions tested in this study. The *dbp1Δ* allele was created by transforming a wild-type haploid with a Cas9 editing plasmid expressing a sgRNA targeted to the *DBP1* ORF alongside a linear repair template that deletes the *DBP1* ORF. This haploid was backcrossed to wild-type yeast and subsequent haploids were mated to create a diploid. Internal tags were inserted between N-terminal 220 and 221 amino acids of Dbp1 and between N-terminal 213 and 214 amino acids of Ded1.

Mitotic growth conditions—For all mitotic growth experiments except for the tethering assays, yeast were grown in rich media (YPD 2% dextrose). Unless otherwise specified, cells were grown overnight at 30°C then back diluted to 0.05 OD_{600} on the day of the experiment and grown until they reached exponential growth rates ~0.6 OD_{600} For meiotic experiments, cells were grown as previously described in Powers et al.[60] For serial dilution experiments, cells were grown overnight or for the indicated length of time shaking at 30°C. Cells were diluted to 0.2 OD_{600} then serially diluted 1:5 and 3uL of cells from each dilution were loaded onto plates.

mRNA tethering assay—Each helicase of interest was C-terminally tagged with the lambda N RNA-binding domain, to tether it specifically to a YFP mRNA containing the boxB binding site (within the 3′ UTR; Reynaud et al.[49]). Helicase fusions were also tagged with BFP and the 3xFLAG peptide sequence so their expression could be monitored. CEN plasmids encoding these constructs and marked with the S. pombe HIS5 allele for selection were transformed into a diploid strain of the BY background which contained heterozygous constructs expressing either YFP including the boxB sequence, or mCherry (with no boxB sequence) integrated at the *URA3* locus. Two independent transformants containing each helicase tether construct were then grown overnight, and then diluted to 0.1 OD_{600} the next day. Once the cells had grown to 0.6 OD_{600}, samples were fixed in 4% paraformaldehyde for 20 min at room temperature for flow cytometry or incubated in 5% trichloroacetic acid overnight at 4°C for western blot analysis. All strains were grown in SC-His and at 30°C. Plasmid constructs can be found in File S6. For meiotic experiments, the BY strain expressing the YFP or mCherry constructs was backcrossed 3 times to wild-type yeast of the SK1 background. The resulting strain of mostly SK1 background had the same YFP and mCherry constructs as used in the vegetative experiments and was transformed with helicase expression constructs. Transformants were grown overnight in SC-His, diluted to 0.25 OD_{600} in BYTA and grown overnight again, then diluted into SPO media at 1.9 OD_{600}. After 4.5h in SPO, western blot samples were collected as described above to assess helicase abundance, and after 5h in SPO samples were collected for flow cytometry as described above.

Western blotting—Samples were prepared by TCA precipitation and extraction. Strains were grown in specified media and 2 or 3.3 OD_{600} equivalents of cells were collected for vegetative and meiotic cultures, respectively. Samples were incubated in 5% TCA for ≥10 min at 4°C then spun down, washed once with TE, once with acetone, then dried overnight. Pellets were resuspended in 150ul of lysis buffer (50 mM Tris-HCl, 1 mM EDTA, 3 mM DTT, 1.1 mM PMSF (Sigma), and 1X cOmplete mini EDTA-free protease inhibitor cocktail

(Roche)) and cells were lysed by bead-beating for 5 min at RT. SDS loading buffer was added to 1X and samples were incubated at 50°C for 10 min and beads were pelleted by centrifugation. Samples were run on a 4–12% Bis-Tris gel at 160V for 5 min followed by 200V for 25 min. Transfer to nitrocellulose membrane was performed using a semi-dry transfer system (Trans-Blot Turbo, BioRad) with a standard 30 min transfer. The membrane was blocked in 5% milk PBS-T or Intercept Blocking Buffer (LiCor Bio) for 1 h at RT and incubated in primary antibody overnight at 4°C. Primary antibodies were diluted in 5% milk in PBS-T + 0.01% sodium azide (mouse anti-V5 (1:2,000; Invitrogen R960–25) and rat anti-tubulin (1:10,000, Serotec, RRID:AB_325005), mouse anti-Ub (1,2000; Santa Cruz sc-8017), and rabbit anti-hexokinase (1:10,000; Rockland 100–4159). Membrane was washed 3X in PBS-T then incubated in secondary antibody (1:15,000 anti-mouse 800 and anti-rabbit 680 in LI-COR PBS blocking buffer) for 1 h at RT, then washed 3X in PBS-T before imaging on the LI-COR Odyssey Imager. Analysis and quantification was performed using ImageStudio Lite software.

Ribosome profiling and polysome profiling—Ribosome profiling and polysome analysis was performed as in.[60] Briefly, cells were treated with cycloheximide for 30s then filtered and flash frozen. Extracts were milled under cryogenic temperatures and stored at −80°C in aliquots. RNA extracted from monosomes was extracted and fragments ~28–32nt were collected. Libraries were prepped using linker ligation and rRNA fragments were depleted from samples using biotinylated anti rRNA oligos. Samples were sequenced using 50nt single end reads on a HS4000or using 50nt single end reads on a NovaSeq 6000. Matched mRNA-seq libraries were prepared with the same library prep protocol with the following changes. Poly A selection was used to isolate mRNA from extracted total RNA samples which were subsequently fragmented and libraries were created with fragments ~35–80nt. No rRNA depletion was performed on these samples.

mRNA-seq and ribosome profiling analysis—Adaptor sequences were trimmed off reads which were then aligned to the yeast genome as previously described in (Cheng et al.[47]). Reads per ORF were counted and RPKMs were calculated for each gene by normalizing the raw reads to the sum of reads per sample and the gene length. Differential expression analysis was performed on raw read counts using DESeq2. Genes with a $P_{adjusted}$ value of less than or equal to .05 were considered significantly different between samples. Sequencing data shown in scatterplots represents the average of 2 or 3 biological replicates with all data shown. For GO analysis for Figures 2S and 5S, based on DESeq2 analysis, significantly regulated genes were split into those upregulated or downregulated in the Dbp1 expressing strains compared to their Ded1 expressing partner. The top 5 enriched GO terms for each category are reported for these analyses. Hierarchical clustering was performed using Cluster 3.0[56] and Java Treeview[57] was used for visualization. For metagene analysis, fragment lengths were analyzed and analysis was performed on samples with characteristic fragment distribution (29mers>28mers). FP reads were normalized to total mapped reads for each sample. Over- or under-digested samples were not analyzed as we found that this impacts the results of metagene analysis for biological replicates. It is important to compare samples with similar fragment distributions.

Analysis of meiotic progression—Cells were prepared to undergo meiosis as described in.[60] For analysis of meiotic divisions, cells were collected at the noted time-points by overnight treatment with 3.7% formaldehyde at 4°C. Cells were resuspended in KPi buffer (100 mM potassium phosphate, pH 6.4) and adhered to poly-L-lysine treated glass slides and membranes were permeabilized by brief treatment of 70% ethanol on slide. Ethanol was aspirated and when wells were dry VectaShield Antifade Mounting Medium with DAPI (Vector Labs) was added. Slides were sealed with a coverslip and used to count nuclei.

Mass spectrometry of mono/polysomes—Extract used for total protein quantification in[42] was subjected to sucrose gradient fractionation and approximately 6 mL of material was collected per sample, containing the monosome/80S and polysome fractions were collected. This was done on biological replicate samples for all 10 conditions analyzed. Proteins were processed by the FASP protocol.[61] Briefly, 100 µL of sample was mixed with 400 µL 8M Guanidine Hydrochloride, then loaded onto a Nanosep Omega 10K column and spun at 14,000g till dry. Then the sample was washed twice with 400 µL Urea Buffer (8 M Urea, 50 mM Tris/HCl (pH8), 75 mM NaCl, 1 mM EDTA) and spun till dry. 100 µL Urea Buffer was added. Disulfide bonds were reduced with 5 mM dithiothreitol and cysteines were subsequently alkylated with 10 mM iodoacetamide. Afterward the samples were spun till dry and 200 µL of 1:4 diluted (dilute with 50 mM Tris/HCl (pH8)) urea buffer was added together with Trypsin and LysC at a ratio of 1:100 to total protein. The samples were then incubated at 25°C overnight. The column was transferred to a new 1.5 mL Eppendorf tube and the digested sample was collected by a spin at 14,000g. Tryptic peptides were desalted on C18 StageTips according to[62] and evaporated to dryness in a vacuum concentrator. Desalted peptides were labeled with the TMT-10plex mass tag labeling reagent according to the manufacturer's instructions (Thermo Scientific) with small modifications. Briefly, 0.2 units of TMT-10plex reagent was used per 10 µg of sample. Peptides were dissolved in 30 µL of 50 mM HEPESHepes pH 8.5 solution and the TMT-11plex reagent was added in 12.3 µL of MeCN. After 1 h incubation the reaction was stopped with 2.5 µL 5% Hydroxylamine for 15 min at 25°C. Differentially labeled peptides were mixed for each replicate and subsequently desalted on C18 StageTips,[62] evaporated to dryness in a vacuum concentrator and reconstituted in 15 µL of 3% acetonitrile and 0.1% formic acid.

LC-MS/MS analysis on a Q-Exactive HF was performed as previously described (Cheng et al.[47]; Keshishian et al; [63]). Briefly, around 1 µg of total peptides were analyzed on an EASY-nLC 1000 UHPLC system (Thermo Fisher Scientific) coupled via a 20 cm C18 column ID picofrit column (New Objective, Woburn, MA) packed in house with Reprosil-Pur C18 AQ 1.9 µm beads (Dr. Maisch, GmbH, Entringen, Germany) to a benchtop Orbitrap Q Exactive HF Plus mass spectrometer (Thermo Fisher Scientific).

Cycloheximide conditions—Cells grown in YEPD (yeast extract, peptone, dextrose) were treated with cycloheximide to a final concentration of 100ug/mL from a 500X stock in ethanol.

MG132 conditions—Cells grown in YEPD were treated with MG132 to a final concentration of 100uM from a 1000X stock in DMSO.

Ded1 and Dbp1 expression and purification—Ded1 and Dbp1 were cloned into pETMCN-based expression vectors (pMH1540 for Ded1, pMH1928 for Dbp1) with an N-terminal 10xHis-MBP tag, followed by a 3C-cleavage site. The expression plasmids were transformed into chemical competent LEMO21 (DE3) bacteria and a preculture was grown in LB + 1% Glucose at 30°C overnight. The next day, the preculture was diluted to OD_{600} = 0.025 in 2 L TB media, grown at 37°C until OD_{600} = 0.6 and induced with 300 μM IPTG. Bacteria were grown over night at 18°C and collected by centrifugation (15 min, 5000 g) the following morning. Pellets were stored at −80°C.

The bacterial pellets were resuspended in lysis buffer (1000 mM NaCl, 50 mM Tris-HCL pH 8.0, 25 mM imidazole, 10% glycerol, DNase, RNase A, protease inhibitors) and lysed with an Emulsiflex C-5 (Avastin) for 2 min. The lysate was centrifuged for 1 h at 80′000 *rcf* at 4°C and the supernatant filtered using a 0.45 μm filter. The initial affinity capturing step was performed with inhouse-made Ni-IMAC columns on an AEKTA purifier (GE Life Science). The eluted fractions were dialyzed overnight at 4°C into 1000 mM, 50 mM Tris-HCL pH 8.0, 25 mM imidazole, 10% glycerol, 2 mM $MgCl_2$ and 3 mM 2-betamercaptethanol, with cleavage of the 10xHis-MBP tag during dialysis by addition of 3C-protease. Reverse Ni-IMAC was performed after the dialysis to remove the cleaved tags. After size exclusion chromatography into final storage buffer (1000 mM, 50 mM phosphate pH 7.5, 10% glycerol, 2 mM $MgCl_2$ and 3 mM 2-betamercaptethanol) using a HiLoad 16/600 Superdex 200 pg column (Cytiva) on an AEKTA purifier at 4°C with a flow rate of 1 mL/min, the proteins were concentrated to ~300 μM and snap-frozen in small aliquots.

Chemical labeling of Dbp1 and Ded1—The proteins were chemically labeled with Atto565-NHS (ATTO-TAC GmbH) following an adopted version of the manufactures protocol in 2-betamercaptethanol free storage buffer (1000 mM, 50 mM phosphate pH 7.5, 10% glycerol, 2 mM $MgCl_2$). The unbound dye was removed using Zeba Spin Desalting Columns (7K MWCO, 0.5 mL, Thermo Fisher Scientific) and concentrated using Amicon Ultra-0.5 centrifugal filter (10 kDa cutoff, Merck).

***In vitro* condensation assay—**Condensate assays were performed by depositing 2 μL of a 50 μM protein solution in storage buffer (1000 mM, 50 mM phosphate pH 7.5, 10% glycerol, 2 mM $MgCl_2$ and 3 mM 2-betamercaptethanol) spiked with 1% of Atto565-labeled protein at the edge of PhenoPlate 384-well ULA-coated microplates (PerkinElmer) and mixing with 18 μL of a low-salt trigger solution. For the trigger solutions, every condition contained a final concentration of 0.5 mg/mL BSA, 25 mM phosphate buffer at the corresponding pH (6.4 or 7.2) and 2 mM of $MgCl_2$. Additional NaCl, ATP (Roth HN35.4, from a 10 mM stock solution) and poly(U) (Sigma Alderich, P9528–25mg, from a 1 mg/mL stock solution) was added to the trigger solution as indicated (final concentration in the well 100 or 200 mM NaCl, 0 or 2 mM ATP, 0 or 0.05 mg/mL polyU). The plates were centrifuged at 10 *rcf* to settle the condensates and incubated for 45 min at the indicated target temperature before image acquisition. Imaging was performed using an inverted epi-fluorescence microscope (Nikon Ti) equipped with a Spectra X LED light source and a Hamamatsu Flash 4.0 sCMOS camera using a PlanApo 40x air objective and the NIS Elements software in a temperature-regulating chamber.

nanoDSF—Thermophoresis experiments were conducted using a Nanotemper Prometheus NT.48 NanoDSF, with a temperature ramp of 1°C per min, from 20°C to 70°C. Fitting of the thermal unfolding curve was fitted using PR Stability Analysis v1.1 (NANOTEMPERTECH). The protein concentration was 0.5 mg/mL in buffer containing 200 mM NaCl, 25 mM sodium phosphate pH 6.4 or 7.2, 1 mM ATP, 1 mM DTT and 10 μM (U)18 RNA. Experiments were performed in independent triplicates, each with three technical replicates.

FRAP—Strains were grown in YEPD and 1 OD_{600} equivalents of cells were incubated at 37C for 10 min before collection. Cells were resuspended in KPi buffer (100 mM potassium phosphate, pH 6.4), adhered to glass slides coated with 1% agarose (Invitrogen) and then subjected to FRAP analysis with a confocal microscope (Zeiss LSM). Four photographs were acquired before bleaching, and the cells were observed for 85 s after bleaching. The sizes of the photographed and bleached areas were maintained constant. Fluorescence intensity in images was calculated with ImageJ (NIH). The recovery curve for normalized fluorescence intensity was calculated after subtraction of background fluorescence intensity.

QUANTIFICATION AND STATISTICAL ANALYSIS

Quantification and analyses for mass spectrometry—All mass spectra were analyzed with the Spectrum Mill software package v4.0 beta (Agilent Technologies) according to[58] using the yeast Uniprot database (UniProt.Yeast.completeIsoforms.UP000002311.20151220; strain ATCC 204508/S288c). For identification, we applied a maximum FDR of 1% separately on the protein and peptide level and proteins were grouped in subgroup specific manner. We required at least 1 spectral count from a unique peptide for protein identification and for protein quantification per replicate measurement. Note that the S288C UniProt dataset was used, because we are not aware of an equivalently complete protein dataset for SK1, and due to poorer sequencing depth and annotation of this genome relative to the reference, our attempt to create one excluded many proteins. This presumably caused us to miss capture of some proteins for which the quantifiable peptides are not identical in the two strains, but should not cause artifacts in our correlation measurements, because all measurements are relative among timepoints.

Finally, we normalized the Spectrum Mill generated intensities such that at each condition/time point the TMT intensity values added up to exactly 1,000,000, therefore each protein group value can be regarded as a normalized microshare (we did this separately for each replicate for all proteins that were present in that replicate TMT mix).

General statistical analysis—Number of replicates, statistical tests, and *p*p-values are provided in figure legends. Statistical parameters are also summarized here. Figure 1: **p*P-value <0.05; ***p*P-value <0.01 from unpaired Student's t-test. Figures 2A–2C: P-value <0.05 = *, $p < 0.01$ = **, and $p < 0.001$ = *** from unpaired Students t-test. Figure 2E: Padj <0.05 = * by ordinary one-way ANOVA, corrected for multiple comparisons using Dunnett's multiple comparison test. Figure 4: One-way ANOVA corrected for multiple comparisons using Dunnett's multiple comparison test, Padj <0.05 = *, <0.01 = **, <0.001 =

, <0.0001 = *. Figure 5: K-S test. P-value < 1e-6 = ****. Figure 6B: no significance by unpaired Student's t-test. Figure S2H: Ordinary one way ANOVA corrected for multiple comparisons with Dunnett's multiple comparison test and a Padj <.05 = *, Padj <.01 = **, Padj <.001 = ***. Figure S3C: Ordinary one-way ANOVA and corrected for multiple comparisons using Dunnett's multiple comparison test with a Padj <0.05 = *, Padj <0.01 = **. Figures S4G and S4H: Two-tailed t test; P-value <0.05 = *, $p < 0.01$ = **, $p < 0.001$ = ***, and $p < 0.0001$ = ****. Figures S4I and S4J: Ordinary one-way ANOVA corrected for multiple comparisons with Dunnett's multiple comparisons test. P-value <0.05 = *. S5A: One-way ANOVA corrected for multiple comparisons using Dunnett's multiple comparison test with Padj <0.01 = **. S6C: Dunnett's multiple comparison test with *$p < 0.05$, ***$p < 0.001$.

Supplementary Material

Refer to Web version on PubMed Central for supplementary material.

ACKNOWLEDGMENTS

We thank Paige Diamond for sharing the global structure file used for DMS-MaPseq analyses, Joe Lobel for assistance with the tethering assay, and Chris Mugler and BrÜn lab members for manuscript comments. This work was supported by NIH funding to G.A.B. (R35GM134886) and M.J. (R35GM128802). E.N.P. was funded by an NSF predoctoral fellowship and N.K. was funded by an overseas research fellowship from Japan Society for the Promotion of Sciences. C.S. was funded by T32GM008295, T32GM148378, and an NSF predoctoral fellowship. M.H. is funded by the Swiss National Science Foundation (PCEFP3_187052) and the European Research Council (ERC-ST2020 950262). N.T.I. is funded by NIH R01GM130996.

REFERENCES

1. Weis K, and Hondele M (2022). The Role of DEAD-Box ATPases in Gene Expression and the Regulation of RNA–Protein Condensates. Annu. Rev. Biochem. 91, 197–219. 10.1146/annurev-biochem-032620-105429. [PubMed: 35303788]
2. Bohnsack KE, Yi S, Venus S, Jankowsky E, and Bohnsack MT (2023). Cellular functions of eukaryotic RNA helicases and their links to human diseases. Nat. Rev. Mol. Cell Biol. 24, 749–769. 10.1038/s41580-023-00628-5. [PubMed: 37474727]
3. Putnam AA, and Jankowsky E (2013). DEAD-box helicases as integrators of RNA, nucleotide and protein binding. Biochim. Biophys. Acta 1829, 884–893. 10.1016/j.bbagrm.2013.02.002. [PubMed: 23416748]
4. Sharma D, and Jankowsky E (2014). The Ded1/DDX3 subfamily of DEAD-box RNA helicases. Crit. Rev. Biochem. Mol. Biol. 49, 343–360. 10.3109/10409238.2014.931339. [PubMed: 25039764]
5. Andreou AZ, and Klostermeier D (2013). The DEAD-box helicase eIF4A: Paradigm or the odd one out? RNA Biol. 10, 19–32. 10.4161/rna.21966. [PubMed: 22995829]
6. Hinnebusch AG (2014). The scanning mechanism of eukaryotic translation initiation. Annu. Rev. Biochem. 83, 779–812. 10.1146/annurev-biochem-060713-035802. [PubMed: 24499181]
7. Kozak M (1986). Point mutations define a sequence flanking the AUG initiator codon that modulates translation by eukaryotic ribosomes. Cell 44, 283–292. [PubMed: 3943125]
8. Hinnebusch AG (2011). Molecular mechanism of scanning and start codon selection in eukaryotes. Microbiol. Mol. Biol. Rev. 75, 434–467. 10.1128/MMBR.00008-11. [PubMed: 21885680]
9. Brar GA (2016). Beyond the Triplet Code: Context Cues Transform Translation. Cell 167, 1681–1692. 10.1016/j.cell.2016.09.022. [PubMed: 27984720]
10. Guenther U-P, Weinberg DE, Zubradt MM, Tedeschi FA, Stawicki BN, Zagore LL, Brar GA, Licatalosi DD, Bartel DP, Weissman JS, and Jankowsky E (2018). The helicase Ded1p controls

use of near-cognate translation initiation codons in 5' UTRs. Nature 559, 130–134. 10.1038/s41586-018-0258-0. [PubMed: 29950728]

11. Gulay S, Gupta N, Lorsch JR, and Hinnebusch AG (2020). Distinct interactions of eIF4A and eIF4E with RNA helicase Ded1 stimulate translation in vivo. Elife 9, e58243. 10.7554/eLife.58243. [PubMed: 32469309]
12. Gupta N, Lorsch JR, and Hinnebusch AG (2018). Yeast Ded1 promotes 48S translation pre-initiation complex assembly in an mRNA-specific and eIF4F-dependent manner. Elife 7, e38892. 10.7554/eLife.38892. [PubMed: 30281017]
13. Sen ND, Zhou F, Ingolia NT, and Hinnebusch AG (2015). Genome-wide analysis of translational efficiency reveals distinct but overlapping functions of yeast DEAD-box RNA helicases Ded1 and eIF4A. Genome Res. 25, 1196–1205. 10.1101/gr.191601.115. [PubMed: 26122911]
14. Zhou F, Bocetti JM, Hou M, Qin D, Hinnebusch AG, and Lorsch JR (2024). Transcriptome-wide analysis of the function of Ded1 in translation preinitiation complex assembly in a reconstituted in vitro system. bioRxiv, 2023.10.16.562452. 10.1101/2023.10.16.562452.
15. Gao Z, Putnam AA, Bowers HA, Guenther U-P, Ye X, Kindsfather A, Hilliker AK, and Jankowsky E (2016). Coupling between the DEAD-box RNA helicases Ded1p and eIF4A. Elife 5, e16408. 10.7554/eLife.16408. [PubMed: 27494274]
16. Firczuk H, Kannambath S, Pahle J, Claydon A, Beynon R, Duncan J, Westerhoff H, Mendes P, and McCarthy JE (2013). An *in vivo* control map for the eukaryotic mRNA translation machinery. Mol. Syst. Biol. 9, 635. 10.1038/msb.2012.73. [PubMed: 23340841]
17. Hilliker A, Gao Z, Jankowsky E, and Parker R (2011). The DEAD-Box Protein Ded1 Modulates Translation by the Formation and Resolution of an eIF4F-mRNA Complex. Mol. Cell 43, 962–972. 10.1016/j.molcel.2011.08.008. [PubMed: 21925384]
18. Calviello L, Venkataramanan S, Rogowski KJ, Wyler E, Wilkins K, Tejura M, Thai B, Krol J, Filipowicz W, Landthaler M, and Floor SN (2021). DDX3 depletion represses translation of mRNAs with complex 5′ UTRs. Nucleic Acids Res. 49, 5336–5350. 10.1093/nar/gkab287. [PubMed: 33905506]
19. Chuang R-Y, Weaver PL, Liu Z, and Chang T-H (1997). Requirement of the DEAD-Box Protein Ded1p for Messenger RNA Translation. Science 275, 1468–1471. 10.1126/science.275.5305.1468. [PubMed: 9045610]
20. Aryanpur PP, Renner DM, Rodela E, Mittelmeier TM, Byrd A, and Bolger TA (2019). The DEAD-box RNA helicase Ded1 has a role in the translational response to TORC1 inhibition. Mol. Biol. Cell 30, 2171–2184. 10.1091/mbc.E18-11-0702. [PubMed: 31141444]
21. Senissar M, Le Saux A, Belgareh-Touzé N, Adam C, Banroques J, and Tanner NK (2014). The DEAD-box helicase Ded1 from yeast is an mRNP cap-associated protein that shuttles between the cytoplasm and nucleus. Nucleic Acids Res. 42, 10005–10022. 10.1093/nar/gku584. [PubMed: 25013175]
22. Aryanpur PP, Regan CA, Collins JM, Mittelmeier TM, Renner DM, Vergara AM, Brown NP, and Bolger TA (2017). Gle1 Regulates RNA Binding of the DEAD-Box Helicase Ded1 in Its Complex Role in Translation Initiation. Mol. Cell Biol. 37, e00139–17. 10.1128/MCB.00139-17. [PubMed: 28784717]
23. Beckham C, Hilliker A, Cziko A-M, Noueiry A, Ramaswami M, and Parker R (2008). The DEAD-Box RNA Helicase Ded1p Affects and Accumulates in *Saccharomyces cerevisiae* P-Bodies. Mol. Biol. Cell 19, 984–993. 10.1091/mbc.e07-09-0954. [PubMed: 18162578]
24. Hilliker A (2012). Analysis of RNA Helicases in P-Bodies and Stress Granules. In Methods in Enzymology (Elsevier), pp. 323–346. 10.1016/B978-0-12-396546-2.00015-2.
25. Iserman C, Desroches Altamirano C, Jegers C, Friedrich U, Zarin T, Fritsch AW, Mittasch M, Domingues A, Hersemann L, Jahnel M, et al. (2020). Condensation of Ded1p Promotes a Translational Switch from Housekeeping to Stress Protein Production. Cell 181, 818–831.e19. 10.1016/j.cell.2020.04.009. [PubMed: 32359423]
26. Sen ND, Zhang H, and Hinnebusch AG (2021). Down-Regulation of Yeast Helicase Ded1 by Glucose Starvation or Heat-Shock Differentially Impairs Translation of Ded1-Dependent mRNAs. Microorganisms 9, 2413. 10.3390/microorganisms9122413. [PubMed: 34946015]

27. Aryanpur PP, Mittelmeier TM, and Bolger TA (2022). The RNA Helicase Ded1 Regulates Translation and Granule Formation during Multiple Phases of Cellular Stress Responses. Mol. Cell Biol. 42, e0024421. 10.1128/MCB.00244-21. [PubMed: 34723653]
28. Glauninger H, Bard JAM, Wong Hickernell CJ, Airoldi EM, Li W, Singer RH, Paul S, Fei J, Sosnick TR, Wallace EWJ, and Drummond DA (2024). Transcriptome-wide mRNA condensation precedes stress granule formation and excludes stress-induced transcripts. Preprint. 10.1101/2024.04.15.589678.
29. Mateju D, Eichenberger B, Voigt F, Eglinger J, Roth G, and Chao JA (2020). Single-Molecule Imaging Reveals Translation of mRNAs Localized to Stress Granules. Cell 183, 1801–1812.e13. 10.1016/j.cell.2020.11.010. [PubMed: 33308477]
30. Banroques J, Cordin O, Doère M, Linder P, and Tanner NK (2011). Analyses of the Functional Regions of DEAD-Box RNA "Helicases" with Deletion and Chimera Constructs Tested In Vivo and In Vitro. J. Mol. Biol. 413, 451–472. 10.1016/j.jmb.2011.08.032. [PubMed: 21884706]
31. Jamieson DJ, and Beggs JD (1991). A suppressor of yeast *spp81/ded1* mutations encodes a very similar putative ATP-dependent RNA helicase. Mol. Microbiol. 5, 805–812. 10.1111/j.1365-2958.1991.tb00753.x. [PubMed: 1857205]
32. Sen ND, Gupta N, Archer K, S., Preiss T, Lorsch JR, and Hinnebusch AG (2019). Functional interplay between DEAD-box RNA helicases Ded1 and Dbp1 in preinitiation complex attachment and scanning on structured mRNAs in vivo. Nucleic Acids Res. 47, gkz595. 10.1093/nar/gkz595.
33. Floor SN, Condon KJ, Sharma D, Jankowsky E, and Doudna JA (2016). Autoinhibitory Interdomain Interactions and Subfamily-specific Extensions Redefine the Catalytic Core of the Human DEAD-box Protein DDX3. J. Biol. Chem. 291, 2412–2421. 10.1074/jbc.M115.700625. [PubMed: 26598523]
34. Berthelot K, Muldoon M, Rajkowitsch L, Hughes J, and McCarthy JEG (2004). Dynamics and processivity of 40S ribosome scanning on mRNA in yeast. Mol. Microbiol. 51, 987–1001. 10.1046/j.1365-2958.2003.03898.x. [PubMed: 14763975]
35. Banroques J, Doère M, Dreyfus M, Linder P, and Tanner NK (2010). Motif III in Superfamily 2 "Helicases" Helps Convert the Binding Energy of ATP into a High-Affinity RNA Binding Site in the Yeast DEAD-Box Protein Ded1. J. Mol. Biol. 396, 949–966. 10.1016/j.jmb.2009.12.025. [PubMed: 20026132]
36. Banroques J, Cordin O, Doère M, Linder P, and Tanner NK (2008). A Conserved Phenylalanine of Motif IV in Superfamily 2 Helicases Is Required for Cooperative, ATP-Dependent Binding of RNA Substrates in DEAD-Box Proteins. Mol. Cell Biol. 28, 3359–3371. 10.1128/MCB.01555-07. [PubMed: 18332124]
37. Powers EN, Chan C, Doron-Mandel E, Llacsahuanga Allcca L, Kim Kim J, Jovanovic M, and Brar GA (2022). Bidirectional promoter activity from expression cassettes can drive off-target repression of neighboring gene translation. Elife 11, e81086. 10.7554/eLife.81086. [PubMed: 36503721]
38. Broach JR (2012). Nutritional Control of Growth and Development in Yeast. Genetics 192, 73–105. 10.1534/genetics.111.135731. [PubMed: 22964838]
39. Neiman AM (2011). Sporulation in the Budding Yeast *Saccharomyces cerevisiae*. Genetics 189, 737–765. 10.1534/genetics.111.127126. [PubMed: 22084423]
40. Plank M (2022). Interaction of TOR and PKA Signaling in S. cerevisiae. Biomolecules 12, 210. 10.3390/biom12020210. [PubMed: 35204711]
41. Brar GA, Yassour M, Friedman N, Regev A, Ingolia NT, and Weissman JS (2012). High-resolution view of the yeast meiotic program revealed by ribosome profiling. Science 335, 552–557. 10.1126/science.1215110. [PubMed: 22194413]
42. Cheng Z, Otto GM, Powers EN, Keskin A, Mertins P, Carr SA, Jovanovic M, and Brar GA (2018). Pervasive, coordinated protein level changes driven by transcript isoform switching during meiosis. Cell 172, 910–923.e16. [PubMed: 29474919]
43. Churchman LS, and Weissman JS (2011). Nascent transcript sequencing visualizes transcription at nucleotide resolution. Nature 469, 368–373. 10.1038/nature09652. [PubMed: 21248844]

44. Gasch AP, Spellman PT, Kao CM, Carmel-Harel O, Eisen MB, Storz G, Botstein D, and Brown PO (2000). Genomic Expression Programs in the Response of Yeast Cells to Environmental Changes. Mol. Biol. Cell 11, 4241–4257. 10.1091/mbc.11.12.4241. [PubMed: 11102521]
45. Kearse MG, and Wilusz JE (2017). Non-AUG translation: a new start for protein synthesis in eukaryotes. Genes Dev. 31, 1717–1731. 10.1101/gad.305250.117. [PubMed: 28982758]
46. Wang J, Shin B-S, Alvarado C, Kim J-R, Bohlen J, Dever TE, and Puglisi JD (2022). Rapid 40S scanning and its regulation by mRNA structure during eukaryotic translation initiation. Cell 185, 4474–4487.e17. 10.1016/j.cell.2022.10.005. [PubMed: 36334590]
47. Eisenberg AR, Higdon AL, Hollerer I, Fields AP, Jungreis I, Diamond PD, Kellis M, Jovanovic M, and Brar GA (2020). Translation Initiation Site Profiling Reveals Widespread Synthesis of Non-AUG-Initiated Protein Isoforms in Yeast. Cell Syst. 11, 145–160.e5. 10.1016/j.cels.2020.06.011. [PubMed: 32710835]
48. Coller J, and Wickens M (2007). Tethered Function Assays: An Adaptable Approach to Study RNA Regulatory Proteins. In Methods in Enzymology (Elsevier), pp. 299–321. 10.1016/S0076-6879(07)29014-7.
49. Reynaud K, McGeachy AM, Noble D, Meacham ZA, and Ingolia NT (2023). Surveying the global landscape of post-transcriptional regulators. Nat. Struct. Mol. Biol. 30, 740–752. 10.1038/s41594-023-00999-5. [PubMed: 37231154]
50. Cheng Z, Mugler CF, Keskin A, Hodapp S, Chan LY-L, Weis K, Mertins P, Regev A, Jovanovic M, and Brar GA (2019). Small and Large Ribosomal Subunit Deficiencies Lead to Distinct Gene Expression Signatures that Reflect Cellular Growth Rate. Mol. Cell 73, 36–47.e10. 10.1016/j.molcel.2018.10.032. [PubMed: 30503772]
51. Zubradt M, Gupta P, Persad S, Lambowitz AM, Weissman JS, and Rouskin S (2017). DMS-MaPseq for genome-wide or targeted RNA structure probing in vivo. Nat. Methods 14, 75–82. 10.1038/nmeth.4057. [PubMed: 27819661]
52. Hondele M, Sachdev R, Heinrich S, Wang J, Vallotton P, Fontoura BMA, and Weis K (2019). DEAD-box ATPases are global regulators of phase-separated organelles. Nature 573, 144–148. 10.1038/s41586-019-1502-y. [PubMed: 31435012]
53. Desroches Altamirano C, Kang M-K, Jordan MA, Borianne T, Dilmen I, Gnädig M, von Appen A, Honigmann A, Franzmann TM, and Alberti S (2024). eIF4F is a thermo-sensing regulatory node in the translational heat shock response. Mol. Cell 84, 1727–1741.e12. 10.1016/j.molcel.2024.02.038. [PubMed: 38547866]
54. Hollerer I, Powers EN, and Brar GA (2021). Global mapping of translation initiation sites by TIS profiling in budding yeast. STAR Protoc. 2, 100250. 10.1016/j.xpro.2020.100250. [PubMed: 33458709]
55. Higdon AL, Won NH, and Brar GA (2024). Truncated protein isoforms generate diversity of protein localization and function in yeast. Cell Syst. 15, 388–408.e4. 10.1016/j.cels.2024.03.005. [PubMed: 38636458]
56. de Hoon MJL, Imoto S, Nolan J, and Miyano S (2004). Open source clustering software. Bioinforma. Oxf. Engl. 20, 1453–1454. 10.1093/bioinformatics/bth078.
57. Saldanha AJ (2004). Java Treeview–extensible visualization of microarray data. Bioinforma. Oxf. Engl. 20, 3246–3248. 10.1093/bioinformatics/bth349.
58. Mertins P, Qiao JW, Patel J, Udeshi ND, Clauser KR, Mani DR, Burgess MW, Gillette MA, Jaffe JD, and Carr SA (2013). Integrated proteomic analysis of post-translational modifications by serial enrichment. Nat. Methods 10, 634–637. 10.1038/nmeth.2518. [PubMed: 23749302]
59. Love MI, Huber W, and Anders S (2014). Moderated estimation of fold change and dispersion for RNA-seq data with DESeq2. Genome Biol. 15, 550. 10.1186/s13059-014-0550-8. [PubMed: 25516281]
60. Powers EN, and Brar GA (2021). Performing Ribosome Profiling to Assess Translation in Vegetative and Meiotic Yeast Cells. Methods Mol. Biol. 2252, 89–125. 10.1007/978-1-0716-1150-0_4. [PubMed: 33765272]
61. Wiśniewski JR, Zougman A, Nagaraj N, and Mann M (2009). Universal sample preparation method for proteome analysis. Nat. Methods 6, 359–362. 10.1038/nmeth.1322. [PubMed: 19377485]

62. Rappsilber J, Mann M, and Ishihama Y (2007). Protocol for micro-purification, enrichment, pre-fractionation and storage of peptides for proteomics using StageTips. Nat. Protoc. 2, 1896–1906. 10.1038/nprot.2007.261. [PubMed: 17703201]

63. Keshishian H, Burgess MW, Gillette MA, Mertins P, Clauser KR, Mani DR, Kuhn EW, Farrell LA, Gerszten RE, and Carr SA (2015). Multiplexed, Quantitative Workflow for Sensitive Biomarker Discovery in Plasma Yields Novel Candidates for Early Myocardial Injury. Mol. Cell. Proteomics 14, 2375–2393. 10.1074/mcp.M114.046813. [PubMed: 25724909]

Highlights

- Dbp1 is the paralog of Ded1, which performs more poorly than Ded1 in promoting translation
- With heat, cells expressing Dbp1 have stress granules and low translation but continue to grow
- Heat stress reduces Ded1 function, making it ineffective at translating structured mRNAs
- Just an 11-amino-acid disordered region of Ded1 drives the cellular response to heat stress

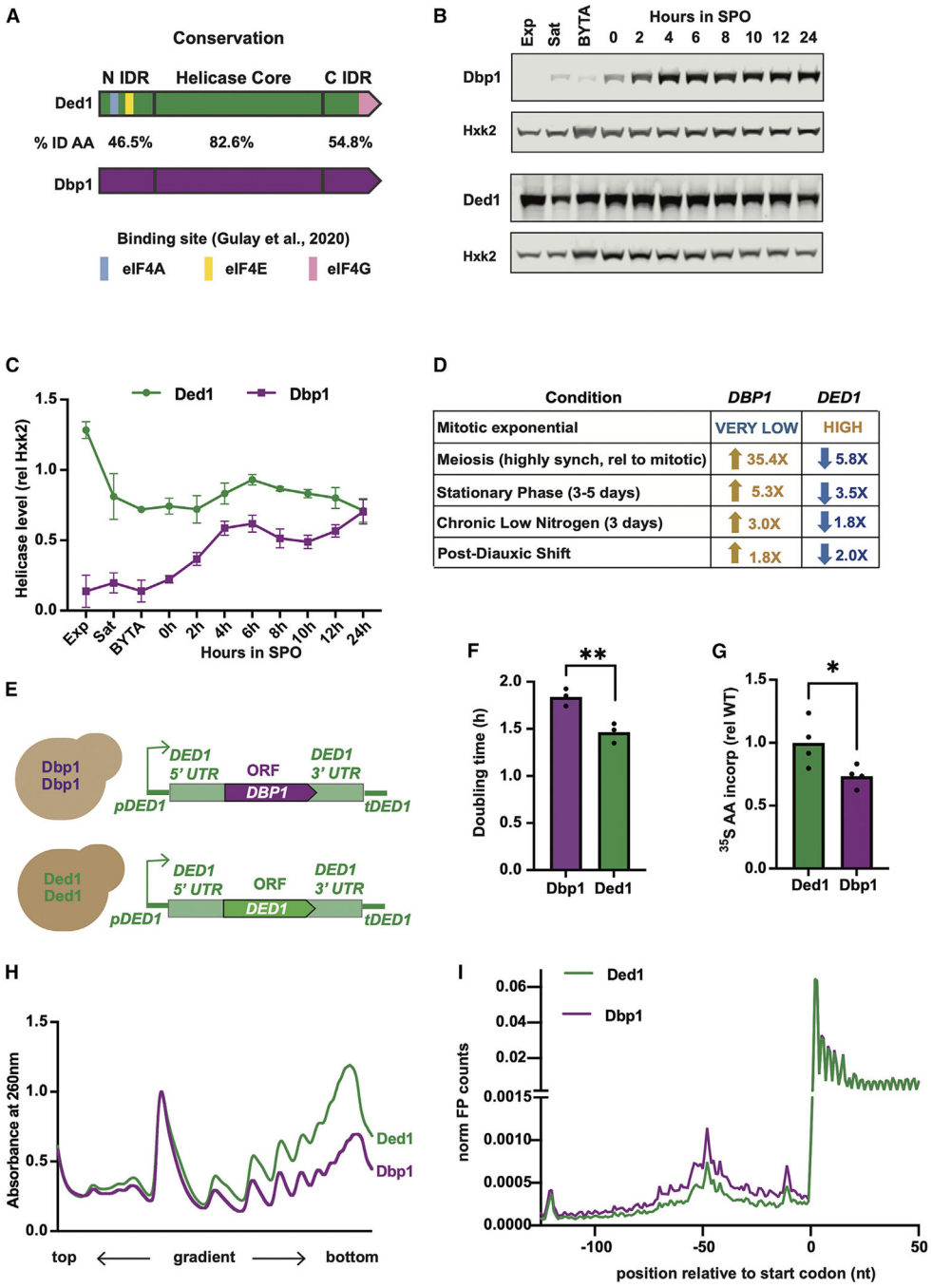

Figure 1. Dbp1 is upregulated and Ded1 is downregulated during meiosis, relative to mitotic growth

(A) Dbp1 and Ded1 amino acid identity by region[30] and known eIF-binding sites.[11,20]

(B) Anti-V5 western blots (WBs) and quantification of cells with internally tagged Ded1 or Dbp1.

(C) Quantification of (B). $N = 3$; data are represented as mean ± SD.

(D) Conditions in which changes in expression of *DBP1* and *DED1* are seen.[41,44]

(E) Schematic of constructs integrated at single-copy and homozygously in diploid cells.

(F) Doubling times for strains in (E), grown in rich medium (YEPD; yeast extract peptone dextrose). $N = 3$; $^{**}p < 0.01$ from unpaired t test.

(G) ^{35}S amino acid incorporation for strains in (E), grown in YEPD in exponential phase. $N = 3$; $^{*}p < 0.05$ from unpaired t test.

(H) Polysome profiles of untagged strains as in (E), matched to S1D. $N = 3$; representative trace shown.

(I) Metagene plots of ribosome footprint (FP) occupancy relative to start codon for untagged strains, as in (E).

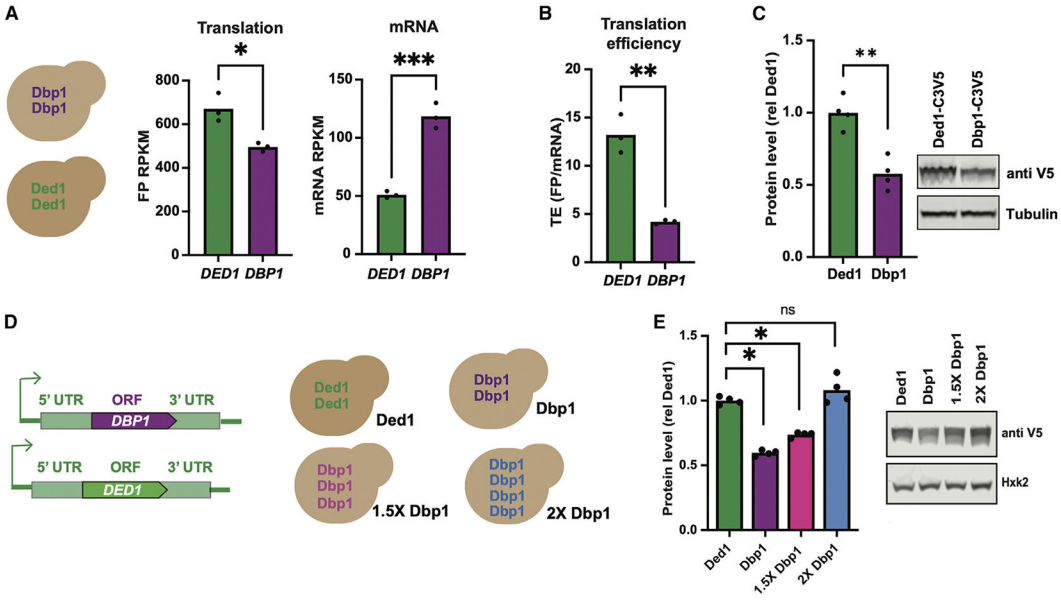

Figure 2. *DBP1* ORF cannot substitute for the *DED1* ORF in supporting robust mitotic growth or translation

(A and B) (A) Translation, mRNA, and (B) translation efficiency (TE; footprint RPKM/mRNA RPKM) of untagged *DBP1*- and *DED1*-expressing cells, as in Figure 1E in exponential growth conditions. $N = 3$; *$p < 0.05$, **$p < 0.01$, and ***$p < 0.001$ by unpaired t test.

(C) Levels of C-terminally 3V5-tagged Ded1 and Dbp1 in exponential growth conditions by WB. $N = 4$; **$p < 0.01$ as determined by unpaired t test.

(D) Schematic of single-copy integrations as in Figures S3A and 1E.

(E) Dbp1/Ded1 protein levels as determined by WB for internally 3V5-tagged strains. Representative blot shown. $N = 4$; *adjusted p ($p$adj) <0.05 by ordinary oneway ANOVA, corrected for multiple comparisons using Dunnett's multiple comparison test.

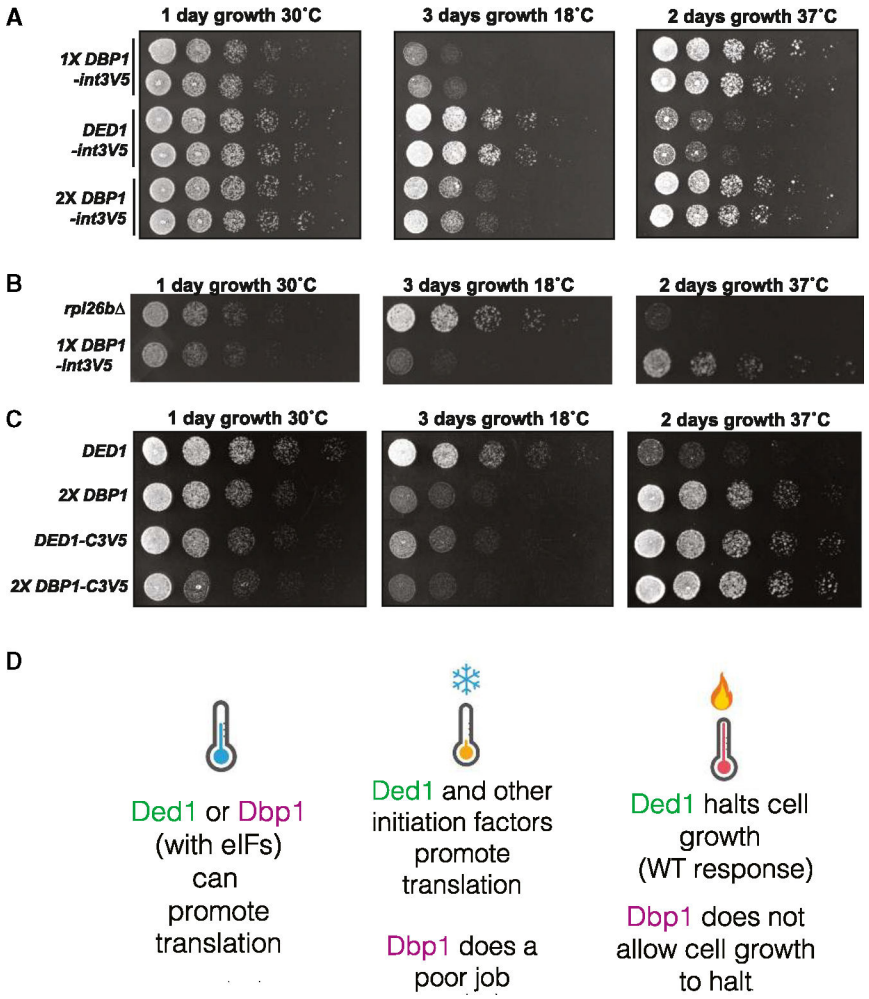

Figure 3. Dbp1 fails to support growth at low temperature and growth reduction at high temperature

Growth of diploid cells on YEPD, with serial 1:5 dilution at 30°C, 18°C, and 37°C.

(A) Internally 3V5-tagged proteins, as in Figure 2E.

(B) Growth-matched *rpl26bΔ* cells and 1× Dbp1 cells in Figure 2E.

(C) Untagged strains expressing matched levels of Ded1 or Dbp1 at top. C-terminal 3V5 tagged strains below. Protein levels in Figures S4I and S4J.

(D) Summary of the ability of Dbp1 and Ded1 to support translation and mitotic growth at different temperatures.

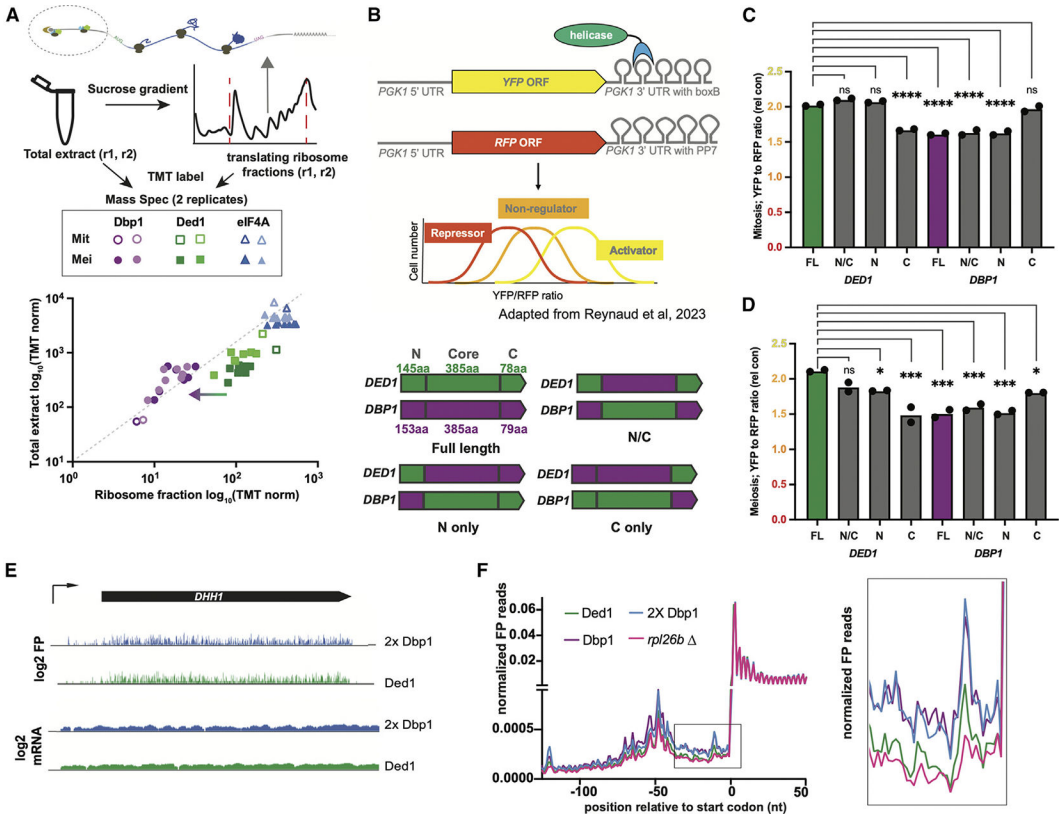

Figure 4. Dbp1 is less effective at driving translation activation than Ded1

(A) Levels of Dbp1, Ded1, and eIF4A that sediment with translating ribosome pools during mitosis or meiosis as determined by TMT mass spectrometry. $N = 2$; matched to experiment in Figure S1A.[42] An example of the species of interest is circled above.

(B) Experimental setup for mRNA tethering assay.[49] Schematics of full-length and chimeric C-terminally tagged proteins below.

(C and D) Mitotic (C) or meiotic (D) cells were analyzed by flow cytometry. $N = 2$; one-way ANOVA corrected for multiple comparisons using Dunnett's multiple comparison test, *$p$adj < 0.05,**$p$adj < 0.01, ***$p$adj < 0.001, ****$p$adj < 0.0001.

(E) Positional data for ribosome footprints (FPs) and mRNA over *DHH1* in mitosis for untagged strains in Figures 2D and S3A.

(F) Metagene plots relative to all annotated start codons for the same strains.

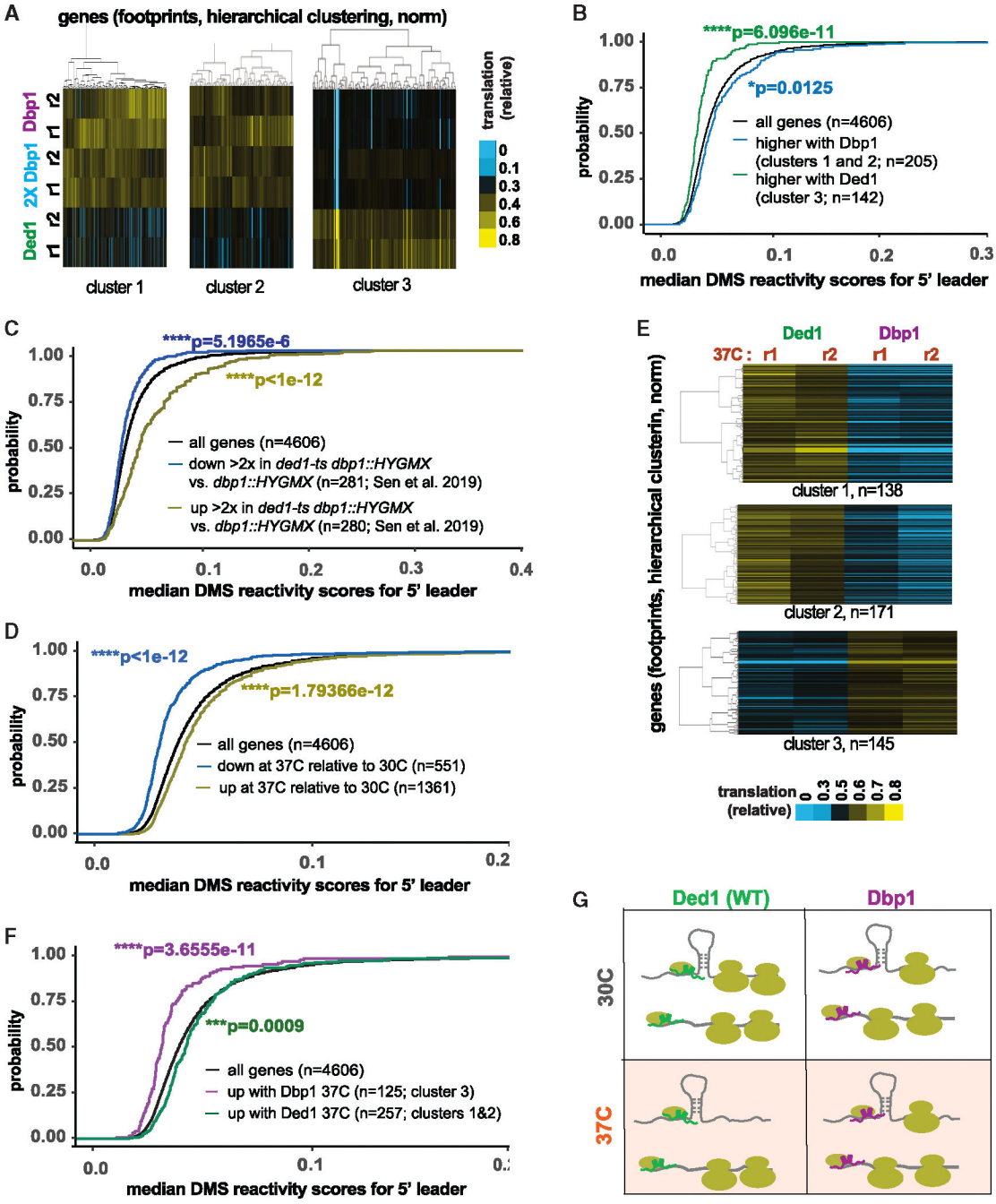

Figure 5. mRNAs with structured 5′ leaders are poorly translated by Dbp1 at 30°C, and even more poorly by Ded1 at 37°C

(A) Ribosome profiling data of untagged strains in Figures 2D and S3A were clustered for all transcripts measured (n = 6,218). The three sub-clusters shown had RNA-remodeler-dependent differences.

(B–D) Median 5′ leader DMS reactivity scores.[51] Significance assessed by K-S test. (B) Analysis of transcripts in (A). (C) Analysis of transcripts up- or downregulated with Ded1 inactivation.[32] (D) Analysis of transcripts in S6A.

(E) Ribosome profiling data for untagged Ded1- vs. Dbp1-expressing cells grown at 37°C were clustered for all transcripts (n = 6,218). The three sub-clusters shown had helicase-dependent differences.

(F) Median 5′ leader DMS reactivity scores[51] for transcripts in (E). Significance by K-S test.

(G) Summary of cytosolic translation of structured transcripts with Ded1 or Dbp1 expression at 30°C vs. 37°C.

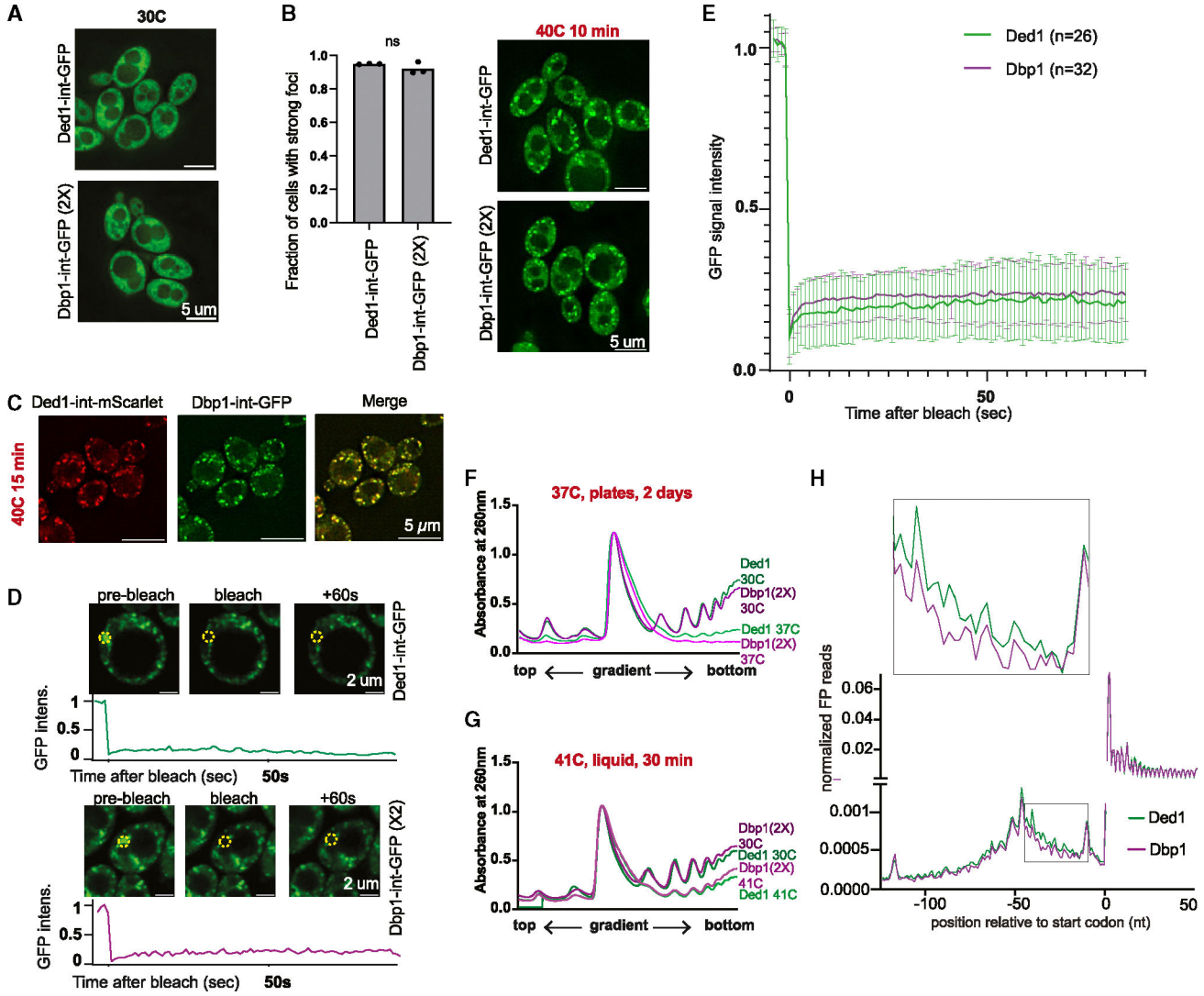

Figure 6. Dbp1- and Ded1-expressing cells form stress granules and reduce bulk translation in response to heat stress

(A and B) Representative images of cells expressing internally GFP-tagged Ded1 or Dbp1 (2×) (A) grown at 30°C or (B) shifted from liquid growth at 30°C to 40°C for 10 min. >100 cells per experiment, quantification at left, N = 3, significance by Student's t test.

(C) Diploid cells expressing internally GFP-tagged Dbp1 and internally mScarlet-tagged Ded1 were imaged after shifting from liquid growth at 30°C to 40°C for 15 min.

(D) FRAP images and traces for cells shifted to 37°C.

(E) Compilation of FRAP data as in (D) for at least 26 cells each; data are represented as mean ± SD.

(F) Representative polysome profiles of Ded1- or Dbp1-expressing cells grown at 30°C or 37°C on YEPD plates.

(G) Representative polysome profiles of Ded1- or Dbp1-expressing cells grown at 30°C or 41°C in liquid YEPD.

(H) Metagene plot relative to all annotated start codons for ribosome profiling data from untagged Dbp1- or Ded1-expressing cells at 37°C.

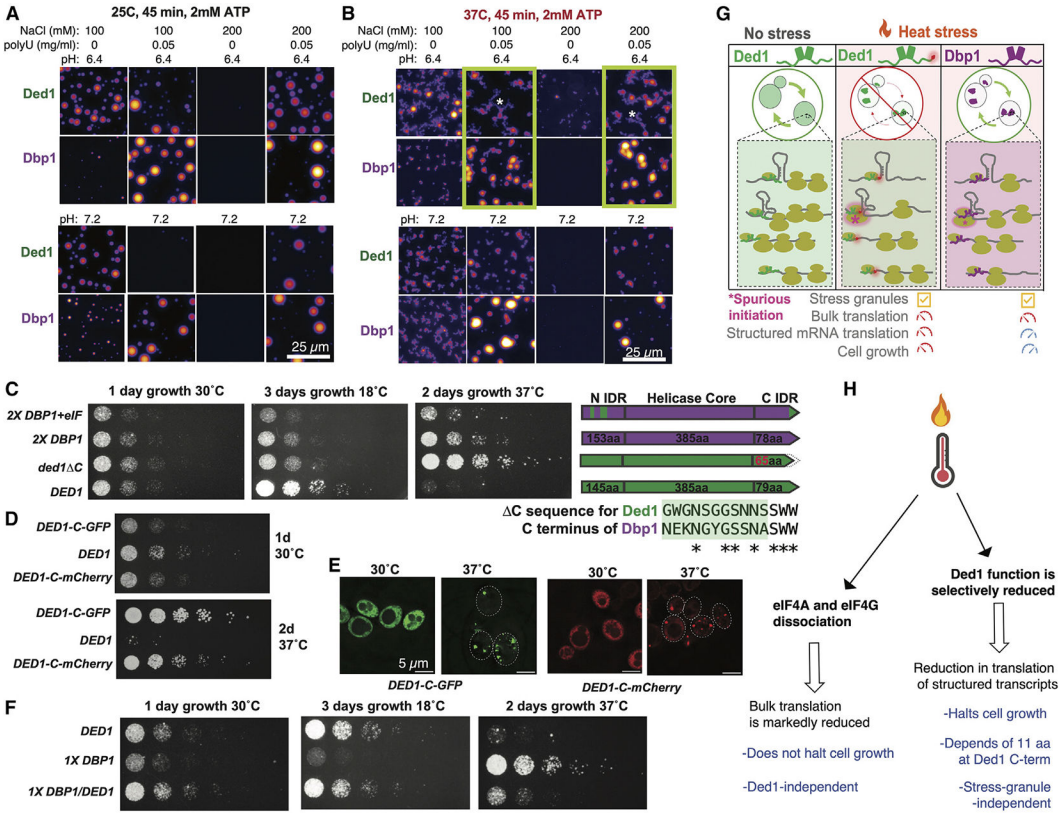

Figure 7. Ded1 undergoes heat-dependent loss in function at high temperature that depends on a short C-terminal region

(A and B) 5 μM purified untagged Ded1 or Dbp1 were imaged in the conditions shown. *N* = 3. In (B), yellow boxes indicate conditions in which Ded1 and Dbp1 morphology differs. Asterisks indicate non-spherical chain-like structures.

(C) 1:5 serial dilution and growth of untagged diploid cells on YEPD plates at either 30°C, 18°C, or 37°C. Untagged strains are shown. Replicate in Figure S6L. Schematics of strains at right, with 14-amino-acid C-terminal sequence shown for Dbp1 and Ded1, with the 11-amino-acid “heat sensor” region of Ded1 in green.

(D) Growth of C-terminally GFP- or mCherry-tagged diploid cells at 30°C or 37°C on YEPD plates, using serial 1:5 dilution, Replicate in Figure S6K.

(E) Microscopy of strains in (D) grown at either 30°C or 37°C.

(F) Growth of untagged diploid cells at 30°C, 18°C, or 37°C on YEPD plates, using serial 1:5 dilution. Replicate in Figure S6L.

(G) Summary of the cellular effects of heat on Ded1, translation, and cell growth.

(H) Summary of proposed two-pronged response to heat shock.

KEY RESOURCES TABLE

REAGENT or RESOURCE	SOURCE	IDENTIFIER
Antibodies		
Anti-V5	Invitrogen	R960–25
Anti-GFP	Clontech	Cat#632381, RRID:AB_2313808
Anti-ubiquitin	Santa cruz bio	Cat#sc-8017, RRID:AB_628423
Anti-tubulin	Serotec	RRID:AB_325005
Anti-hexokinase	Rockland	Cat#100–4159, RRID:AB_2119918
800 secondary	LI-COR	Cat#926–32210, RRID:AB_621842
680 secondary	LI-COR	Cat#926–68071, RRID:AB_10956166
Chemicals, peptides, and recombinant proteins		
cOmplete mini EDTA-free protease inhibitor cocktail	Roche	Cat#29384100
Acid-washed glass beads	Sigma	Cat#G8772
PBS Odyssey Blocking Buffer	LI-COR	Cat#927–40100
Acid phenol, pH4.3	Ambion	Cat#AM9722
PMSF	Sigma	P7626
Superscript III	Thermo	12574026
VectaShield Antifade Mounting Medium with DAPI	Vector labs	H1200–10
Deposited data		
Ribosome profiling of mitotic exponential cells expressing either Dbp1 or Ded1, at 30C or 37C	This paper	GSE262933
Ribosome profiling of mitotic exponential cells expressing either 2XDbp1, 1XDbp1, or Ded1	This paper	GSE262934
Ribosome profiling of WT vs. Cas9-based DBP1 deletion	This paper	GSE262935
Experimental models: Organisms/strains		
All strain genotypes are listed in File S6		
Oligonucleotides		
All oligos listed in File S6		
Recombinant DNA		
Plasmids listed in File S6		
Software and algorithms		
ImageStudio Lite Software	LI-COR	https://www.licor.com/bio/image-studio-lite/

REAGENT or RESOURCE	SOURCE	IDENTIFIER
Cluster 3.0	de Hoon et al.[56]	
Java TreeView	Saldanha et al.[57]	
SpectrumMill	Mertins et al.[58]	
DESeq2	Love et al.[59]	